A vibrant, abstract painting in acrylic on canvas by Mark Chadwick from 2010. The composition features a complex interplay of colors including red, yellow, blue, white, and black, creating a dynamic, swirling, and energetic effect reminiscent of a proton's internal structure.

The proton spin: a tale of one-half

Emanuele R. Nocera

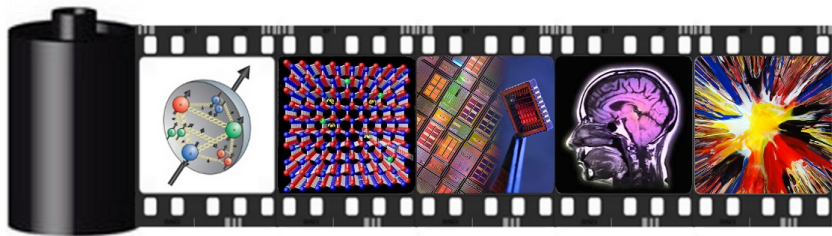
Università di Genova & INFN, Genova

Genova - January 20, 2015

Mark Chadwick, *Abstract Spin Painting 21*, Acrylic on canvas (2010)

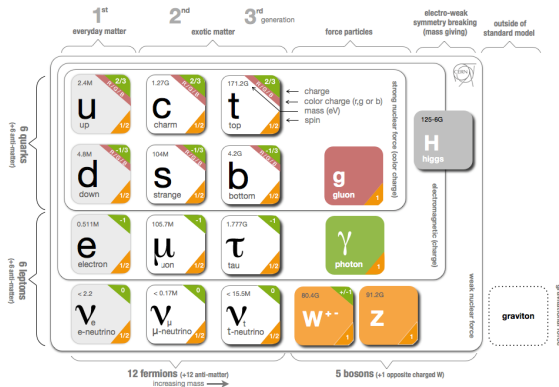
Spin, a fundamental concept in physics

- ➊ SPIN is deeply rooted in the symmetries and structure of space-time
 - ▶ *an intrinsic form of angular momentum*
 - ▶ seminal role in Quantum Mechanics
- ➋ SPIN determines whether a particle follows Fermi or Bose statistics
 - ▶ implications in the structure of matter and the stability of many-body systems
 - ▶ lays the foundations for chemistry and biology
- ➌ SPIN has evident effects even at large scales, almost in everyday life
 - ▶ spintronics-based memory chips
 - ▶ nuclear magnetic resonance imaging



Spin in particle physics

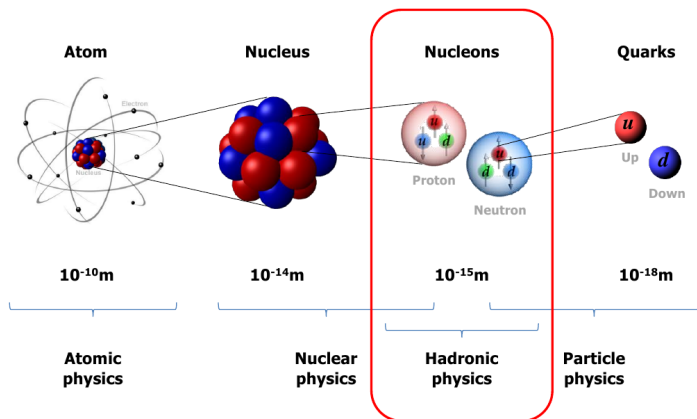
All elementary particles in the SM carry spin, except the recently observed Higgs boson
Among them, the particles that are subject to the strong interactions: quarks and gluons



SPIN is intimately entwined with Quantum Chromodynamics

Spin in hadron physics

Nucleons, protons and neutrons, are bound states with spin one-half
They make up all nuclei and hence most of the visible mass in the Universe



They have internal structure, and such a structure is intimately entwined with SPIN

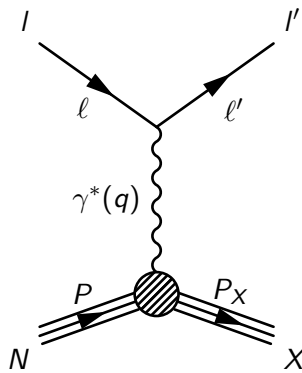
Outline

- ➊ Partons in QCD
 - ▶ Distributions, polarization, and all that
- ➋ A global determination of polarized PDFs
 - ▶ Data, methodology, (most recent) results
- ➌ The path forward
 - ▶ Future opportunities at JLAB, RHIC and EIC
- ➍ Drawing conclusions

1. Partons in QCD

Blake Brasher, *Deep Inelastic Scattering*, Acrylic, ink, and holographic glitter on canvas (2014)

A modern realization of Rutherford's experiment



$$I(\ell) + N(P) \rightarrow I'(\ell') + X(P_X)$$

$$\frac{d^3\sigma^{s_\ell,S}}{dxdy d\varphi} = \frac{\alpha_{em}^2 y}{2Q^4} \left[L_{\mu\nu}^{(S)} W^{\mu\nu(S)} - L_{\mu\nu}^{(A)} W^{\mu\nu(A)} \right]$$

$$L^{\mu\nu} = \sum_{s_{\ell'}} [\bar{u}(\ell, s_\ell) \gamma^\nu u(\ell', s_{\ell'}) \bar{u}(\ell', s_{\ell'}) \gamma^\mu u(\ell, s_\ell)]$$

$$W_{\mu\nu} = \frac{1}{2\pi} \sum_X \int d\Pi_X \left[\langle P, S | J_\nu^\dagger(q) | P_X \rangle \langle P_X | J_\mu(q) | P, S \rangle \right]$$

$$W_{\mu\nu}^{(A)} = \frac{2M\epsilon_{\mu\nu\rho\sigma} q^\rho}{P \cdot q} \left\{ S^\sigma g_1(x) + \left[S^\sigma - \frac{S \cdot q}{P \cdot q} P^\sigma \right] g_2(x) \right\}$$

$$\frac{d^3\sigma^{\rightarrow; \Rightarrow}}{dxdy} - \frac{d^3\sigma^{\rightarrow; \Leftarrow}}{dxdy} = \frac{8\pi\alpha_{em}^2}{Q^2} \left[\left(2 - y - \frac{\gamma^2 y^2}{2} \right) g_1(x) - \gamma^2 y g_2(x) \right], \quad \gamma = x \frac{M}{Q}$$

Helicity-dependent (polarized) parton distribution functions

- ① Asymmetry as an incoherent sum of lepton-parton point-like interactions

$$\frac{d^2\sigma^{\rightarrow;\Rightarrow}}{dxdy} - \frac{d^2\sigma^{\rightarrow;\Leftarrow}}{dxdy} = \sum_q e_q^2 \Delta f(x) \left[\frac{d\hat{\sigma}^{\rightarrow;\rightarrow}}{dy} - \frac{d\hat{\sigma}^{\rightarrow;\Leftarrow}}{dy} \right]$$

- ② The momentum densities of partons with spin (\uparrow) or (\downarrow) w.r.t the nucleon

$$\Delta f(x) \equiv f^\uparrow(x) - f^\downarrow(x), \quad f = u, \bar{u}, d, \bar{d}, s, \bar{s}, g$$

$$\Delta q(x) = \text{Diagram of two red circles with white dots and arrows pointing right} - \text{Diagram of two red circles with black dots and arrows pointing right}$$
$$\Delta g(x) = \text{Diagram of two red circles with three black dots and arrows pointing right} - \text{Diagram of two red circles with three white dots and arrows pointing right}$$

- ③ Allow for a proper field-theoretic definition as matrix elements of bilocal operators

$$\Delta q(x) = \frac{1}{4\pi} \int dy^- e^{-iy^- xP^+} \langle P, S | \bar{\psi}(0, y^-, \mathbf{0}_\perp) \gamma^+ \gamma^5 \psi(0) | P, S \rangle$$

$$\Delta g(x) = \frac{1}{4\pi x P^+} \int dy^- e^{-iy^- xP^+} \langle P, S | G^{+\alpha}(0, y^-, \mathbf{0}_\perp) \tilde{G}_\alpha^+(0) | P, S \rangle$$

with light-cone coordinates and QCD field-strength tensor G ($A^+ = 0$ gauge)

$$y = (y^+, y^-, \mathbf{y}_\perp), \quad y^+ = (y^0 + y^z)/\sqrt{2}, \quad y^- = (y^0 - y^z)/\sqrt{2}, \quad \mathbf{y}_\perp = (v^x, v^y)$$

$$G_{\mu\nu}^\alpha = \partial_\mu A_\nu^\alpha - \partial_\nu A_\mu^\alpha + f^{abc} A_\mu^b A_\nu^c$$

Naive parton model expectations

- ① In the naive parton model, one would expect

$$\frac{d^2\sigma^{+;\Rightarrow}}{dxdy} - \frac{d^2\sigma^{+;\Leftarrow}}{dxdy} = \frac{4\pi\alpha_{em}^2}{Q^2} \left[\sum_q e_q^2 \Delta q(x) (2-y) \right]$$

- ② In terms of structure functions (assuming $n_f = 3$)

$$g_1^P(x) = \frac{1}{2} \sum_q e_q^2 \Delta q(x) = \frac{1}{9} \Delta \Sigma(x) + \frac{1}{12} \Delta T_3(x) + \frac{1}{36} \Delta T_8(x) \quad g_2^P(x) = 0$$

$$\Delta \Sigma = \Delta u^+ + \Delta d^+ + \Delta s^+ \quad \Delta T_3 = \Delta u^+ - \Delta d^+ \quad \Delta T_8 = \Delta u^+ + \Delta d^+ - 2\Delta s^+$$

- ③ Relate the first moment of $\Delta \Sigma$ to the m.e. of the flavor singlet axial current

$$a_0 = \langle P, S | J_\Sigma^{\hat{z}} | P, S \rangle = \int_0^1 dx \Delta \Sigma(x) = 2 \langle S^{q+\bar{q}} \rangle \approx 1$$

- ④ European Muon Collaboration result (1988)

$$a_0 = 0.098 \pm 0.076 \pm 0.113$$

The EMC experiment and the *proton spin crisis*



Physics Letters B

Volume 206, Issue 2, 19 May 1988, Pages 364–370



A measurement of the spin asymmetry and determination of the structure function g_1 in deep inelastic muon-proton scattering

European Muon Collaboration

Volume 206, number 2

PHYSICS LETTERS B

19 May 1988

The spin asymmetry in deep inelastic scattering of longitudinally polarised muons by longitudinally polarised protons has been measured over a large x range ($0.01 < x < 0.7$). The spin-dependent structure function $g_1(x)$ for the proton has been determined and its integral over x found to be $0.114 \pm 0.012 \pm 0.026$, in disagreement with the Ellis-Jaffe sum rule. Assuming the validity of the Bjorken sum rule, this result implies a significant negative value for the integral of g_1 for the neutron. These values for the integrals of g_1 lead to the conclusion that the total quark spin constitutes a rather small fraction of the spin of the nucleon.

The EMC experiment and the *proton spin crisis*



Nuclear Physics B

Volume 328, Issue 1, 11 December 1989, Pages 1–35



An investigation of the spin structure of the proton in deep inelastic scattering of polarised muons on polarised protons

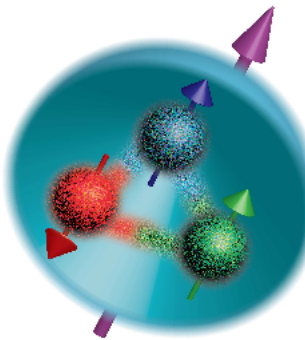
The European Muon Collaboration

J. Ashman et al. / Spin structure of proton

The spin asymmetry in deep inelastic scattering of longitudinally polarised muons by longitudinally polarised protons has been measured in the range $0.01 < x < 0.7$. The spin dependent structure function $g_1(x)$ for the proton has been determined and, combining the data with earlier SLAC measurements, its integral over x found to be $0.126 \pm 0.010(\text{stat.}) \pm 0.015(\text{syst.})$, in disagreement with the Ellis–Jaffe sum rule. Assuming the validity of the Bjorken sum rule, this result implies a significant negative value for the integral of g_1 for the neutron. These integrals lead to the conclusion, in the naïve quark parton model, that the total quark spin constitutes a rather small fraction of the spin of the nucleon. Results are also presented on the asymmetries in inclusive hadron production which are consistent with the above picture.

A realistic (QCD) picture of the nucleon

naive picture



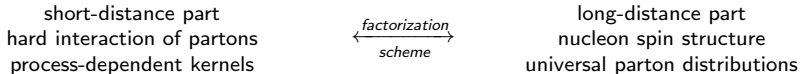
three non-relativistic quarks

\longleftrightarrow *QCD*
factorization, evolution

indefinite number of relativistic
quarks and gluons

Factorization of physical observables

- ① A variety of sufficiently inclusive processes allow for a factorized description



- ② Physical observables are written as a convolution of coefficient functions and PDFs

$$\mathcal{O}_I = \sum_{f=q,\bar{q},g} \Delta C_{If}(y, \alpha_s(\mu^2)) \otimes \Delta f(y, \mu^2) \quad f \otimes g = \int_x^1 \frac{dy}{y} f\left(\frac{x}{y}\right) g(y)$$

- ③ Coefficient functions allow for a perturbative expansion

$$\Delta C_{If}(y, \alpha_s) = \sum_{k=0} a_s^k \Delta C_{If}^{(k)}(y), \quad a_s = \alpha_s/(4\pi)$$

- ④ For the structure function g_1 one has (at leading twist)

$$g_1(x, \mu^2) = \frac{\langle e^2 \rangle}{2} [\Delta C_{NS} \otimes \Delta q_{NS} + \Delta C_S \otimes \Delta \Sigma + 2n_f \Delta C_g \otimes \Delta g] \quad \langle e^2 \rangle = n_f^{-1} \sum_{i=1}^{n_f} e_i^2$$

$$\Delta q_{NS} \equiv \sum_{i=1}^{n_f} \left(\frac{e_i^2}{\langle e^2 \rangle} - 1 \right) [\Delta q_i + \Delta \bar{q}_i] \quad \Delta \Sigma \equiv \sum_{i=1}^{n_f} [\Delta q_i + \Delta \bar{q}_i]$$

$$\Delta C_{NS}^{(0)} = \Delta C_S^{(0)} = \delta(1-x) \quad \Delta C_g^{(0)} = 0$$

Scale-dependence of PDFs: DGLAP equations

- ① A set of $(2n_f + 1)$ integro-differential equations, n_f is the number of active flavors

$$\frac{\partial}{\partial \ln \mu^2} \Delta f_i(x, \mu^2) = \sum_j^{n_f} \int_x^1 \frac{dz}{z} \Delta P_{ji}(z, \alpha_s(\mu^2)) \Delta f_j\left(\frac{x}{z}, \mu^2\right)$$

- ② Often written in a convenient basis of PDFs

$$\Delta q_{NS;\pm} = (\Delta q_i \pm \Delta \bar{q}_i) - (\Delta q_j \pm \Delta \bar{q}_j) \quad \Delta q_{NS;v} = \sum_i^{n_f} (\Delta q_i - \Delta \bar{q}_i) \quad \Delta \Sigma = \sum_i^{n_f} (\Delta q_i + \Delta \bar{q}_i)$$

$$\frac{\partial}{\partial \ln \mu^2} \Delta q_{NS;\pm,v}(x, \mu^2) = P^{\pm,v}(x, \mu_F^2) \otimes \Delta q_{NS;\pm,v}(x, \mu^2)$$

$$\frac{\partial}{\partial \ln \mu^2} \begin{pmatrix} \Delta \Sigma(x, \mu^2) \\ \Delta g(x, \mu^2) \end{pmatrix} = \begin{pmatrix} \Delta P^{qq} & \Delta P^{gq} \\ \Delta P^{qg} & \Delta P^{gg} \end{pmatrix} \otimes \begin{pmatrix} \Delta \Sigma(x, \mu^2) \\ \Delta g(x, \mu^2) \end{pmatrix}$$

- ③ With perturbative computable splitting functions (computed up to NNLO)

$$\Delta P_{ji}(z, \alpha_s) = \sum_{k=0} a_s^{k+1} \Delta P_{ji}^{(k)}(z), \quad a_s = \alpha_s/(4\pi)$$



The proton helicity sum rule

- ① A decomposition of the nucleon spin

$$\frac{1}{2} = \frac{1}{2}\Delta\Sigma(\mu^2) + \Delta G(\mu^2) + \mathcal{L}_q(\mu^2) + \mathcal{L}_g(\mu^2)$$

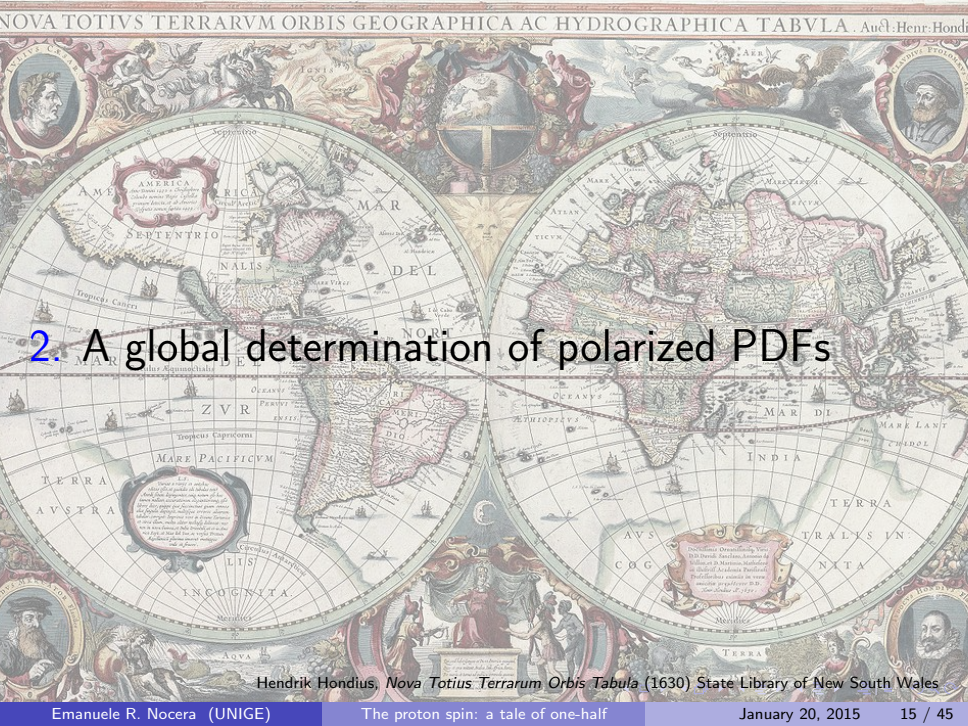
$$\Delta\Sigma(\mu^2) = \sum_{q=u,d,s} \int_0^1 [\Delta q(x, \mu^2) + \Delta \bar{q}(x, \mu^2)] \quad \Delta G(\mu^2) = \int_0^1 dx \Delta g(x, \mu^2)$$

- ② All $\Delta\Sigma$, ΔG , \mathcal{L}_q and \mathcal{L}_g depend on the factorization scale μ (and scheme)
- ③ Beyond LO, the axial charge reads

$$a_0 = \Delta\Sigma(\mu^2) - n_f \frac{\alpha_s(\mu^2)}{2\pi} \Delta G(\mu^2)$$

- ④ According to DGLAP equations, ΔG evolves as $[\alpha_s(\mu^2)]^{-1}$
- ⑤ The gluon decouples from g_1 , the naive parton model predictions are not recovered
- ⑥ Depending on ΔG there may be a cancellation with $\Delta\Sigma$ leading to $a_0 \approx 0$

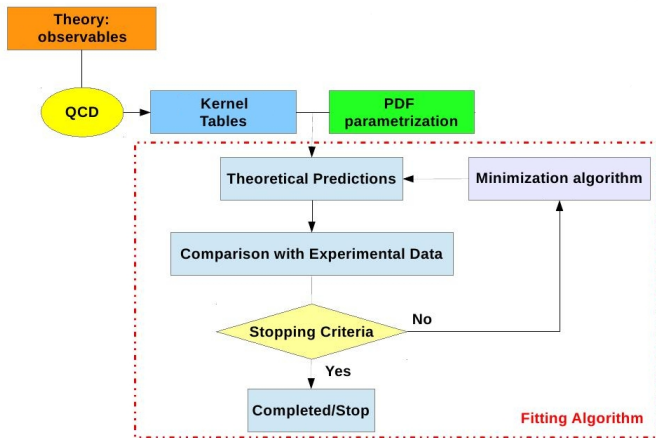
The rest of the talk will be on the determination of $\Delta\Sigma(\mu^2)$ and $\Delta G(\mu^2)$ in the $\overline{\text{MS}}$ factorization scheme at NLO accuracy



2. A global determination of polarized PDFs

Hendrik Hondius, *Nova Totius Terrarum Orbis Tabula* (1630) State Library of New South Wales

Anatomy of a global QCD analysis of PDFs



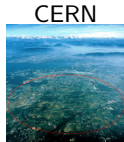
Obtain PDFs through global minimization of a figure of merit (e.g. χ^2)

Determine the set of best-fit parameters entering the assumed PDF parametrization

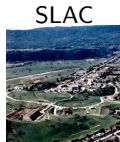
Need for a prescription to estimate and propagate uncertainties

Experimental data

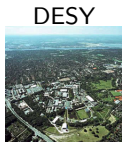
Process	Reaction	Subprocess	PDFs probed	x	$Q^2/p_T^2/M^2 [\text{GeV}^2]$
	$\ell^\pm \{p, d, n\} \rightarrow \ell^\pm X$	$\gamma^* q \rightarrow q$	$\frac{\Delta q + \Delta \bar{q}}{\Delta g}$	$0.003 \lesssim x \lesssim 0.8$	$1 \lesssim Q^2 \lesssim 70$
	$\ell^\pm \{p, d\} \rightarrow \ell^\pm hX$	$\gamma^* q \rightarrow q$	$\frac{\Delta u + \Delta \bar{u}}{\Delta d + \Delta \bar{d}}$ $\frac{\Delta g}{\Delta g}$	$0.005 \lesssim x \lesssim 0.5$	$1 \lesssim Q^2 \lesssim 60$
	$\ell^\pm \{p, d\} \rightarrow \ell^\pm DX$	$\gamma^* g \rightarrow c\bar{c}$	Δg	$0.06 \lesssim x \lesssim 0.2$	~ 10
	$\vec{p} \vec{p} \rightarrow jet(s)X$	$gg \rightarrow qg$ $qg \rightarrow qg$	Δg	$0.05 \lesssim x \lesssim 0.2$	$30 \lesssim p_T^2 \lesssim 800$
	$\vec{p} p \rightarrow W^\pm X$	$u_L d_R \rightarrow W^+$ $d_L \bar{u}_R \rightarrow W^-$	$\Delta u + \Delta \bar{u}$ $\Delta d + \Delta \bar{d}$	$0.05 \lesssim x \lesssim 0.4$	$\sim M_W^2$
	$\vec{p} \vec{p} \rightarrow \pi X$	$gg \rightarrow qg$ $qg \rightarrow qg$	Δg	$0.05 \lesssim x \lesssim 0.4$	$1 \lesssim p_T^2 \lesssim 200$



EMC, SMC, COMPASS



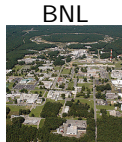
E142, E143, E154, E155



HERMES



HALL-A, CLAS



PHENIX, STAR

DIS&SIDIS

A few issues

- ① Limited (x, Q^2) kinematic coverage
 - ▶ difficult to get Δg from scaling violations in DIS and SIDIS
 - additional *direct* probes of Δg are needed (jets, open-charm)
 - ▶ need to use data down to $Q^2 = 1 \text{ GeV}^2$
 - is perturbative QCD reliable?
 - how much higher twists affect the perturbative description of observables?
 - ② No neutrino DIS data
 - ▶ no quark-antiquark separation from inclusive DIS
 - limited set of W^\pm production data in $p\bar{p}$ collisions
 - SIDIS data require knowledge of fragmentation functions (extra uncertainties)
-

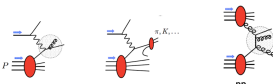
- ① Relate the octet of axial-vector currents to β -decay of spin-1/2 hyperons

$$a_3 = \int_0^1 dx \Delta T_3 = F + D = 1.2701 \pm 0.0025 \quad a_8 = \int_0^1 dx \Delta T_8 = 3F - D = 0.585 \pm 0.025$$

- ② Require the positivity of cross sections

$$|g_1(x, \mu^2)| \leq F_1(x, \mu^2) \stackrel{\text{LO}}{\Longleftrightarrow} |\Delta f(x, \mu^2)| \leq f(x, \mu^2)$$

Recent determinations of polarized PDFs (\sim past 4 years)



collaboration	DIS	SIDIS	PP	latest update	features
DSSV	☒	☒	☒ (jets, π^0)	[arXiv:1404.4293]	global fit
NNPDF	☒	☒	☒ (jets, W^\pm)	[arXiv:1406.5539]	minimally biased fit
JAM	☒	☒	☒	[arXiv:1310.3734]	large- x effects
LSS	☒	☒	☒	[arXiv:1010.0574]	higher-twist effects
BB	☒	☒	☒	[arXiv:1005.3113]	simultaneous fit of α_s

+ simultaneous determination of PDF uncertainties

N.B.: PDF uncertainties stem from three sources

- ① the underlying data, affected by statistical and (correlated) systematic errors
- ② the theory used to describe them, based on the truncation of a perturbative series
- ③ the procedure used to determine PDFs from data

Available PDF sets are all based on item 2, but may differ significantly for items 1 and 3

Methodological detour: the standard methodology

① Simple analytical parametrization of PDFs

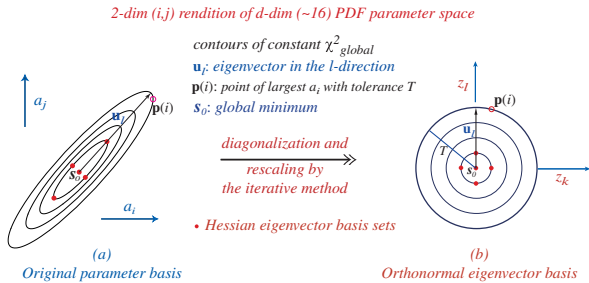
$$x \Delta f_i(x, \mu_0^2) = \eta_i x^{a_i} (1-x)^{b_i} \left(1 + \rho_i x^{\frac{1}{2}} + \gamma_i x \right)$$

⇒ potential bias if the parametrization is too rigid

② Hessian propagation of errors

- ▶ expand the χ^2 about its global minimum at first order
- ▶ diagonalize the Hessian matrix and take the hypersphere of radius $\sqrt{\Delta\chi^2} = 1$

⇒ is linear approximation adequate? do we need a tolerance $T = \sqrt{\Delta\chi^2} > 1$?



Methodological detour: the NNPDF methodology

① Neural network parametrization of PDFs

- ▶ redundant and flexible parametrization, $\mathcal{O}(200)$ parameters
- ▶ requires a proper minimization algorithm and stopping criterion

⇒ **reduce the theoretical bias due to the parametrization**

② Monte Carlo propagation of errors

- ▶ generate experimental data replicas assuming multi-Gaussian probability distribution
- ▶ validate against experimental data to determine the sample size ($N_{\text{rep}} \sim 100$)

⇒ **no need to rely on linear error propagation, no tolerance needed**

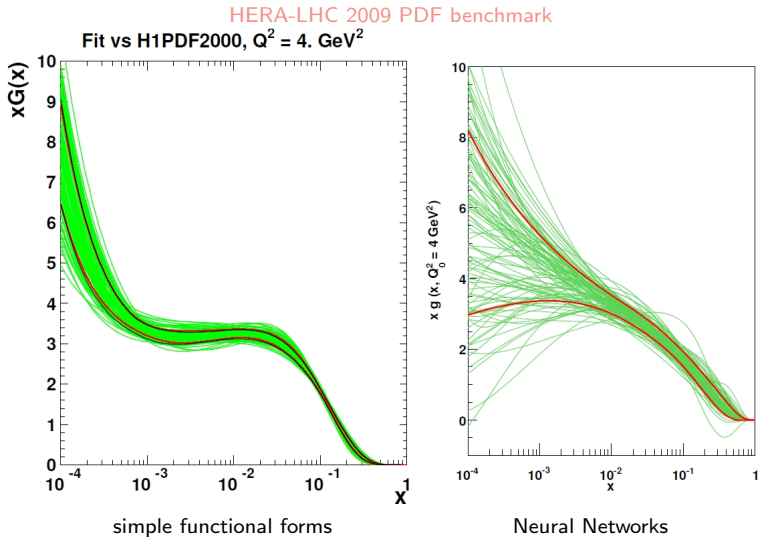
PDF replicas are equally probable members of a **statistical ensemble** which samples the probability density $\mathcal{P}[f_i]$ in the space of PDFs

$$\langle \mathcal{O} \rangle = \int \mathcal{D}f_i \mathcal{P}[f_i] \mathcal{O}[f_i]$$

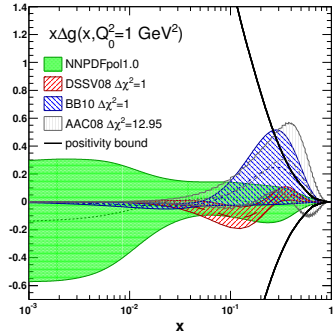
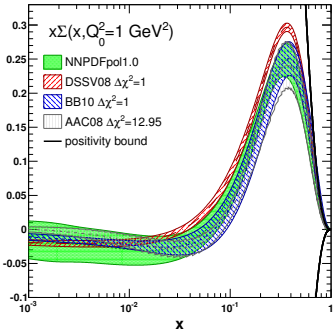
Expectation values for observables are **Monte Carlo integrals**

$$\langle \mathcal{O}[f_i(x, Q^2)] \rangle = \frac{1}{N_{\text{rep}}} \sum_{k=1}^{N_{\text{rep}}} \mathcal{O}[f_i^{(k)}(x, Q^2)]$$

Methodological detour: potential consequences



Polarized PDFs from DIS: status 2013



$$\int_{0.001}^1 dx \Delta \Sigma(x, Q_0^2) = +0.25 \pm 0.09$$

$$\int_0^1 dx \Delta \Sigma(x, Q_0^2) = +0.22 \pm 0.20$$

$$\int_{0.001}^1 dx \Delta g(x, Q_0^2) = -0.26 \pm 0.19$$

$$\int_0^1 dx \Delta g(x, Q_0^2) = -1.2 \pm 4.2$$

Two new analyses in 2014

DSSV++ [1404.9293]

Δg update of DSSV08 [0804.0422]

PRL 113, 012001 (2014)

PHYSICAL REVIEW LETTERS

March 2014

5

Evidence for Polarization of Gluons in the Proton

Daniel de Florian^a and Rodolfo Sassot^b

Departamento de Física y IFIBA, Facultad de Ciencias Exactas y Naturales, Universidad de Buenos Aires,
Cuidad Universitaria, Pabellón 1 (1428) Buenos Aires, Argentina

Marcus Steinmann^c

Institute for Theoretical Physics, Tübingen University, Auf der Morgenstelle 14, 72076 Tübingen, Germany
and Physics Department, Brookhaven National Laboratory, Upton, New York 11973, USA

Werner Vogelsang^d

Institute for Theoretical Physics, Tübingen University, Auf der Morgenstelle 14, 72076 Tübingen, Germany
(Received 17 April 2014; published 2 July 2014)

We discuss the impact of recent high-statistics Relativistic Heavy Ion Collider data on the determination of the gluon polarization in the proton in the context of a global QCD analysis of polarized parton distributions. We find evidence for a nonvanishing polarization of gluons in the region of momentum fraction and at all scales mostly probed by the data. Although information from low momentum fractions is presently lacking, this finding is suggestive of a significant contribution of gluon spin to the proton spin, thereby leaving the amount of orbital angular momentum required to balance the proton spin budget.

DOI: 10.1103/PhysRevLett.113.012001

PACS numbers: 13.88.+e, 12.38.Bx, 13.60.Bb, 13.85.Ni

Introduction.—The gluon helicity distribution function $\Delta g(x)$ of the proton has long been recognized as a fundamental quantity characterizing the inner structure of the nucleon. In particular, its integral $\Delta G = \int_0^1 dx \Delta g(x)$ of all gluons in the proton is believed to be zero [1]. The light-cone gauge interpretation of the gluon spin contributes to the proton spin [1]. As such, ΔG is a key ingredient to the proton helicity sum rule

$$\frac{1}{2} - \frac{1}{2} \Delta \Sigma + \Delta G + L_g + L_{\bar{g}} \quad (1)$$

where $\Delta \Sigma$ denotes the combined quark and antiquark spin contributions and L_g and $L_{\bar{g}}$ the quark and gluon orbital angular momentum contributions. For simplicity, we have omitted the renormalization scale Q and scheme dependence of all quantities.

It is well known that the quark and gluon helicity distributions can be probed in high-energy scattering processes with particle-antiparticle annihilation or creation and $\Delta \Sigma$ and ΔG . Experiments on polarized deep-inelastic lepton-nucleon scattering (DIS) performed since the late eighties [2] have shown that relatively little of the proton spin is carried by the quark and antiquark spins, with a typical value of -0.125 [2–4]. The inclusive DIS asymmetries have been interpreted as gluon spinless. Instead, the best probes of Δg are offered by polarized proton-proton collisions at the BNL Relativistic Heavy Ion Collider (RHIC) [5]. Several processes in $p\bar{p}$ collisions, in particular jet or hadron production at high transverse momentum p_T , receive substantial contributions

from gluon-induced hard scattering, hence, opening a window on Δg when polarized probe beams are used.

The first round of results produced by RHIC until 2007 [5] were in conflict with data from inclusive semi-inclusive DIS at the NAL and CERN (NLC) global QCD analysis [3], hereafter referred to as “DSSV analysis”. One of the main results of that analysis was that the RHIC data—within their uncertainties at the time—did not show any evidence of a polarization of gluons inside the proton. In fact, the integrated Δg over the range $0.05 \leq x \leq 0.2$ of momentum fraction primarily accessed by the RHIC experiments was found to be very close to zero. Other recent analyses of nucleon spin structure [4] did not fully include RHIC data; as a result Δg was left largely unconstrained.

Since the analysis [3], the data from RHIC have vastly improved. New results from the 2009 run [6,7] at center-of-mass energy $\sqrt{s} = 200$ GeV have significantly smaller errors across the range of measured p_T . This will naturally put tighter constraints on $\Delta g(x)$ and extend the range of momenta where constraints can be imposed.

A striking feature is that the STAR jet data [6] now exhibit a double-spin asymmetry A_{LL} that is clearly nonvanishing over the whole range $5 \leq p_T \leq 30$ GeV, in contrast to the previous results. Keeping in mind that in this regime, jets are primarily produced by gluon-gluon and quark-gluon annihilation, one might expect the gluon inside the proton might be polarized. At the same time, new PHENIX data for x^2 production [7] still do not show any significant asymmetry, and it is of course important to reveal whether the two data sets provide compatible information. In this Letter, we assess the impact of the 2009 RHIC data sets on

NNPDFpol1.1 [1406.5539]

Δg , $\Delta \bar{q}$ update of NNPDFpol1.0 [1303.7236]



Available online at www.sciencedirect.com

ScienceDirect



Nuclear Physics B 887 (2014) 276–308

www.sciencedirect.com/science/journal/nuclphysb

A first unbiased global determination of polarized PDFs and their uncertainties

NNPDF Collaboration

Emanuele R. Nocera^a, Richard D. Ball^a, Stefano Forte^{b,*},
Giovanni Ridolfi^c, Juan Rojo^{d,e}

^a Higgs Centre, University of Edinburgh, JCMB, KB, Marischal Rd, Edinburgh EH9 3JZ, Scotland, United Kingdom

^b Dipartimento di Fisica, Università di Milano and INFN, Sezione di Milano, Via Celoria 16, I-20133 Milano, Italy

^c INFN, Sezione di Genova, Genova, Italy

^d CERN, CH-1211 Geneva 23, Switzerland

^e Rudolf Peierls Centre for Theoretical Physics, 1 Keble Road, University of Oxford, OX1 3NP Oxford, United Kingdom

Received 25 June 2014; received in revised form 17 August 2014; accepted 18 August 2014

Available online 22 August 2014

Editor: Tommy Ohlsson

Abstract

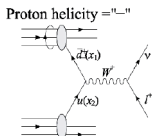
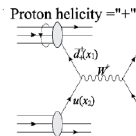
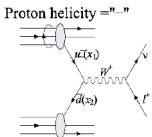
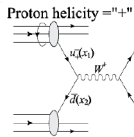
We present a first global determination of spin-dependent parton distribution functions (PDFs) and their uncertainties using the NNPDF methodology. NNPDFpol1.1 . Longitudinally polarized hard-inclusive scattering data, already used for the previous NNPDFpol1.0 PDF set, are supplemented with the most recent polarized hadron collider data for inclusive jet and W boson production from the STAR and PHENIX experiments at RHIC, and with open-charm production data from the COMPASS experiment, thereby allowing for a separate determination of the polarized quark and antiquark PDFs, and an improved determination of the momenta and large- x polarized gluon PDF. We study the phenomenological implications of the NNPDFpol1.1 set, and we provide predictions for the longitudinal double-spin asymmetry for semi-inclusive pion production at RHIC.

© 2014 CERN for the benefit of the NNPDF Collaboration. Published by Elsevier B.V. This is an open access article under the CC BY license (<http://creativecommons.org/licenses/by/3.0/>). Funded by SCOPA³.

* Corresponding author.

<https://doi.org/10.1016/j.nuclphysb.2014.08.008>
0550-3213/14 © 2014 CERN for the benefit of the NNPDF Collaboration. Published by Elsevier B.V. This is an open access article under the CC BY license (<http://creativecommons.org/licenses/by/3.0/>). Funded by SCOPA³.

New data from RHIC: W^\pm production

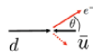


$$A_L^{W^-} \sim$$

$$\frac{\Delta \bar{u}_{x_1} d_{x_2} (1 - \cos \theta)^2 - \Delta d_{x_1} \bar{u}_{x_2} (1 + \cos \theta)^2}{\bar{u}_{x_1} d_{x_2} (1 - \cos \theta)^2 - d_{x_1} \bar{u}_{x_2} (1 + \cos \theta)^2}$$



backward lepton rapidity



forward lepton rapidity

Longitudinal single- and double-spin asymmetries

$$A_L = \frac{\sigma^+ - \sigma^-}{\sigma^+ + \sigma^-} \quad A_{LL} = \frac{\sigma^{++} - \sigma^{+-}}{\sigma^{++} + \sigma^{+-}}$$

FEATURES

- quark/antiquark separation at $Q \sim M_W$
- no need of fragmentation functions
- at RHIC, $\langle x_{1,2} \rangle \simeq \frac{M_W}{\sqrt{s}} e^{-\eta l/2} \approx [0.04, 0.4]$
- for W^+ , $d \longleftrightarrow u$ and $\Delta d \longleftrightarrow \Delta u$
- non-trivial positivity bound [arXiv:1104.2920]

$$1 \pm A_{LL}(y_W) > |A_L(y_W) \pm A_L(-y_W)|$$

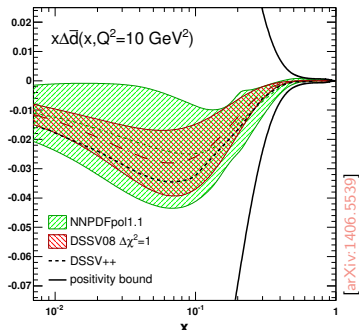
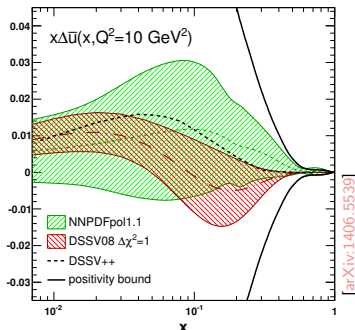
- no access to strangeness ($W^\pm + c$ required)

MEASUREMENTS

- STAR [arXiv:1404.6880] + PHENIX [PoS(DIS2014)205]
- much more to come from ongoing RHIC run

New data from RHIC: W^\pm production

EFFECTS ON THE LIGHT QUARK SEA POLARIZATION $\Delta\bar{u}$ AND $\Delta\bar{d}$

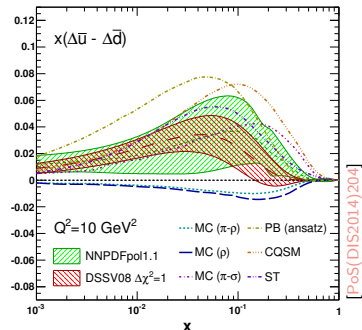
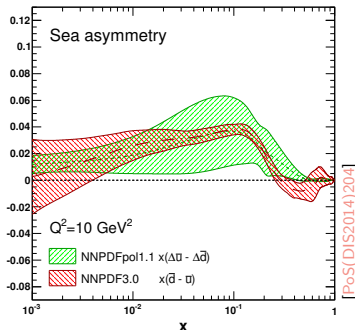


NNPDFpol1.1: SIDIS , W^\pm ; DSSV08: SIDIS , W^\pm ; DSSV++: SIDIS , W^\pm

$Q^2 = 10 \text{ GeV}^2$	$\int_0^1 dx \Delta f(x, Q^2)$		$\int_{10^{-3}}^1 dx \Delta f(x, Q^2)$		
	NNPDFpol1.0	NNPDFpol1.1	NNPDFpol1.0	NNPDFpol1.1	DSSV08
$\Delta\bar{u}$	—	$+0.06 \pm 0.06$	—	$+0.04 \pm 0.05$	$+0.028^{+0.059}_{-0.059}$
$\Delta\bar{d}$	—	-0.11 ± 0.06	—	-0.09 ± 0.05	$-0.089^{+0.090}_{-0.080}$

New data from RHIC: W^\pm production

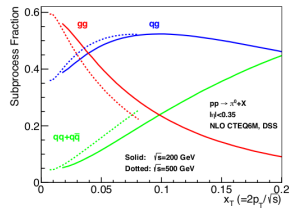
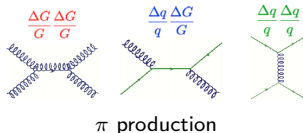
EFFECTS ON THE FLAVOR ASYMMETRY $\Delta\bar{u} - \Delta\bar{d}$



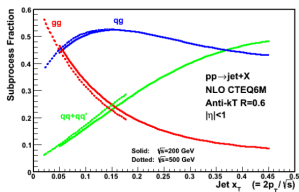
$$I_\Delta(Q^2) = \int_0^1 dx \left[\Delta\bar{u}(x, Q^2) - \Delta\bar{d}(x, Q^2) \right], \quad Q^2 = 10 \text{ GeV}^2$$

I_Δ	MC (π -meson) $\equiv 0$	MC (ρ -meson) < 0	PB (bag-model) $\simeq 0.09$	PB $\simeq 0.2$	IN $\simeq 0.2$	DSSV08 $\Delta\chi^2 = 1$ 0.14 ± 0.05
I_Δ	MC (π - ρ inter.) $[-4 \cdot 10^{-3}, -0.033]$	MC (π - σ inter.) $\simeq 0.12$	PB (ansatz) $\simeq 0.3$	CQS 0.31	ST > 0.12	NNPDFpol1.1 0.17 ± 0.08

New data from RHIC: jet and π production



Jet production



Longitudinal double-spin asymmetry

$$A_{LL} = \frac{\sigma^{++} - \sigma^{+-}}{\sigma^{++} + \sigma^{+-}}$$

FEATURES

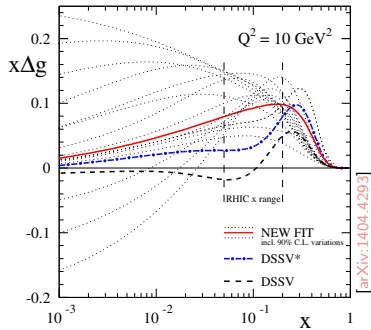
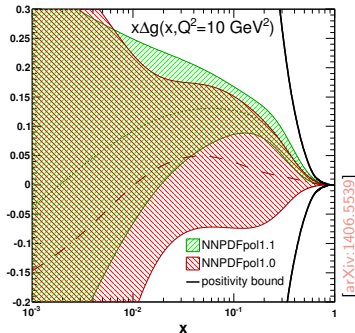
- at RHIC, $\langle x_{1,2} \rangle \simeq \frac{2p_T}{\sqrt{s}} e^{-\eta/2} \approx [0.05, 0.2]$
- qg** and **gg** initiated subprocesses dominate (for most of the RHIC kinematics)
- A_{LL} sensitive to gluon polarization
- cross sections are well described at NLO in pQCD

MEASUREMENTS

- STAR (jets) [[arXiv:1405.5134](#)]
- PHENIX (π) [[arXiv:1402.6296](#)] [[arXiv:1409.1907](#)]
- much more to come from ongoing RHIC run
 - gaining precision
 - di-jet measurements

New data from RHIC: jet and π production

EFFECTS ON THE GLUON POLARIZATION Δg



NNPDFpol1.0: jets \boxtimes , π \boxtimes ;

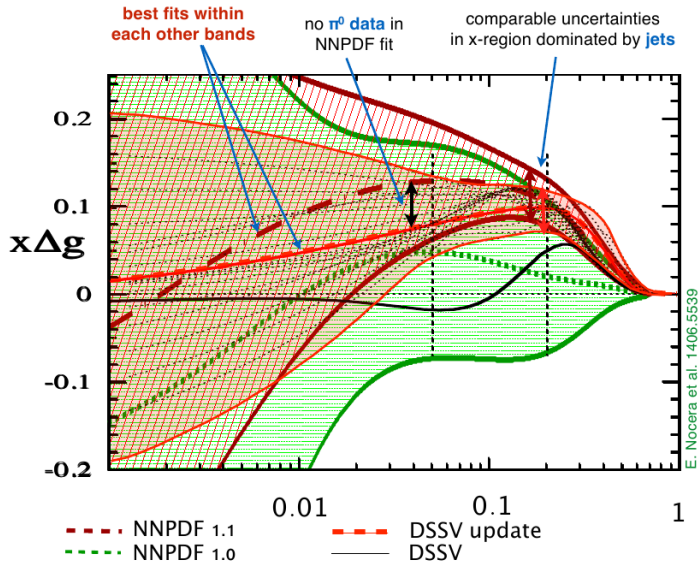
NNPDFpol1.1: jets \boxdot , π \boxtimes ;

DSSV++: jets \boxdot , π \boxdot ;

$Q^2 = 10 \text{ GeV}^2$	$\int_0^1 dx \Delta g(x, Q^2)$	$\int_{10^{-3}}^1 dx \Delta g(x, Q^2)$	$\int_{0.05}^{0.2} dx \Delta g(x, Q^2)$
NNPDFpol1.0	-0.95 ± 3.87	-0.06 ± 1.12	$+0.05 \pm 0.15$
NNPDFpol1.1	-0.13 ± 2.60	$+0.31 \pm 0.77$	$+0.15 \pm 0.06$
DSSV08	—	$0.013^{+0.702}_{-0.314}$	$0.005^{+0.129}_{-0.164}$
DSSV++	—	—	$0.10^{+0.06}_{-0.07}$

New data from RHIC: jet and π production

EFFECTS ON THE GLUON POLARIZATION Δg



First evidence of gluon polarization in the proton



First evidence of gluon polarization in the proton

SCIENTIFIC
AMERICAN™

Sign In | Register  0

Subscribe to All Access »

Subscribe to Print »

Give a Gift »

View the Latest Issue »

Subscribe

News & Features

Topics

Blogs

Videos & Podcasts

Education

Citizen Science

SA Magazine

SA Mind

Books

SA en español

[More Science](#) » [News](#)

 19 ::  Email ::  Print

Proton Spin Mystery Gains a New Clue



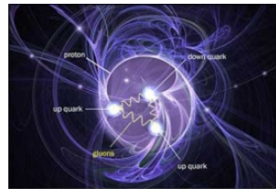
Physicists long assumed a proton's spin came from its three constituent quarks. New measurements suggest particles called gluons make a significant contribution



July 21, 2014 | By Clara Moskowitz



Protons have a constant spin that is an intrinsic particle property like mass or charge. Yet where this spin comes from is such a mystery it's dubbed the "proton spin crisis." Initially physicists thought a proton's spin was the sum of the spins of its three constituent quarks.



First evidence of gluon polarization in the proton

Mail Online



Home | News | U.S. | Sport | TV&Showbiz | Australia | Femail | Health | **Science** | Money | Video | Travel | Fashion Finder

Science Home | Pictures | Gadgets Gifts and Toys Store

Login

Mystery of 'proton spin' solved? Particle collider reveals that quarks AND gluons may hold answer to great subatomic puzzle

- Researchers using a collider in New York say they have solved 'spin' mystery
- Since an experiment in 1987 the origins of proton spin have been unknown
- It had once been thought to be cause exclusively by quarks
- But this was proved to be wrong in the failed experiment 27 years ago
- Now a new study says gluons play an important role in proton spin
- Could bring to a close one of the greatest mysteries of subatomic physics

By JONATHAN O'CALLAGHAN

PUBLISHED: 14:23 GMT, 22 July 2014 | UPDATED: 14:37 GMT, 22 July 2014

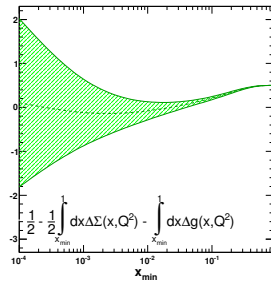
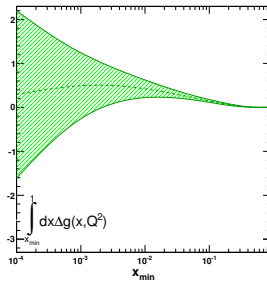
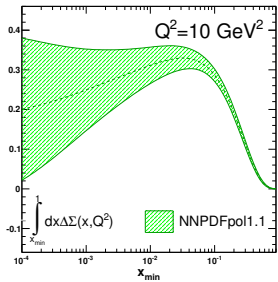


41
View comments



The spin content of the proton

$$\frac{1}{2} = \frac{1}{2} \int_0^1 dx \Delta \Sigma(x, Q^2) + \int_0^1 dx \Delta g(x, Q^2) + \mathcal{L}_q + \mathcal{L}_g$$



quarks and antiquarks $\sim 20\% - 30\%$

gluons $\sim 70\%$

OAM $\sim 0\%$

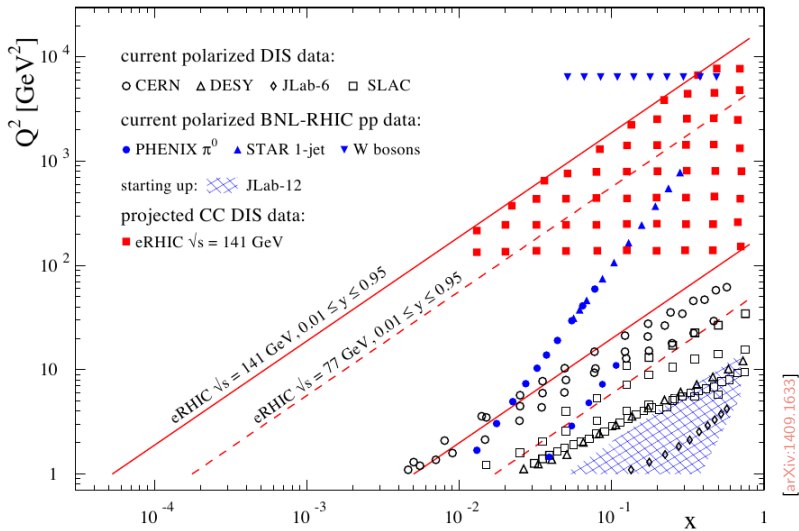
BUT LARGE UNCERTAINTIES \iff NEED FOR DATA

An abstract painting featuring a winding path made of small, glowing yellow and white dots. The path starts from the bottom left, curves upwards and to the right, and then descends towards the center. The background is composed of soft, blended colors in shades of blue, purple, and yellow, creating a dreamlike atmosphere.

3. The path forward

Luiza Vizali, *Path through the sky*, Acrylic, metallic acrylic, stretched canvas (2008)

Need for experimental data



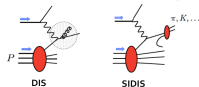
Ongoing/planned/proposed experimental programs

Jefferson Laboratory



Physics Opportunities with
the 12 GeV Upgrade at Jefferson Lab

[arXiv:1208.1244]

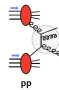


large- x , high precision

Relativistic
Heavy Ion Collider

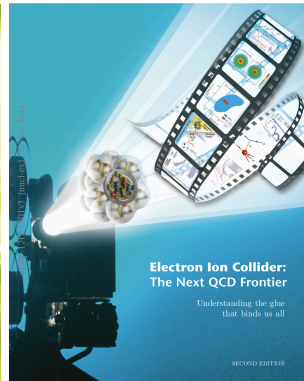


[arXiv:1501.01220]



Δg , Δq , $\Delta \bar{q}$

A future
Electron-Ion Collider

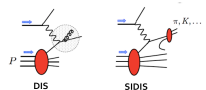


Electron Ion Collider:
The Next QCD Frontier

Understanding the glue
that binds us all

SECOND EDITION

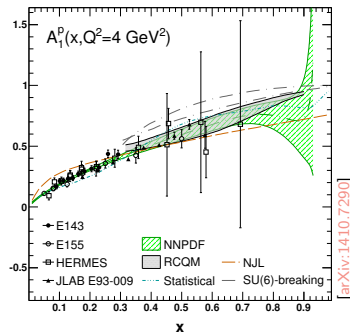
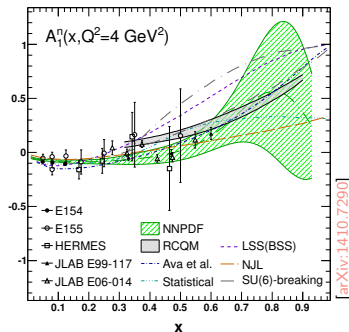
[arXiv:1212.1701]



small- x , high- Q^2

Opportunities at JLAB (towards 12 GeV upgrade)

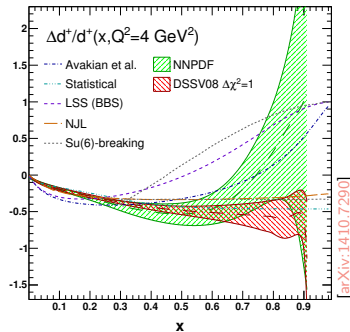
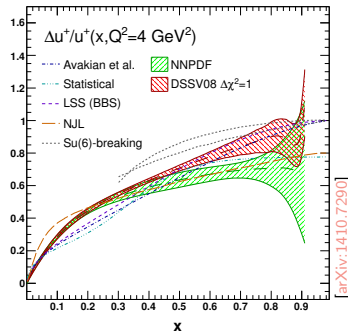
VIRTUAL PHOTOABSORPTION ASYMMETRY IN INCLUSIVE DIS



Model	A_1^n	A_1^p	Model	A_1^n	A_1^p
SU(6)	0	$5/9$	NJL	0.35	0.77
RCQM	1	1	DSE (<i>realistic</i>)	0.17	0.59
QHD ($\sigma_{1/2}$)	1	1	DSE (<i>contact</i>)	0.34	0.88
QHD (ψ_ρ)	1	1	pQCD	1	1
NNPDF ($x = 0.7$)	0.41 ± 0.31	0.75 ± 0.07	NNPDF ($x = 0.9$)	0.36 ± 0.61	0.74 ± 0.34

Opportunities at JLAB (towards 12 GeV upgrade)

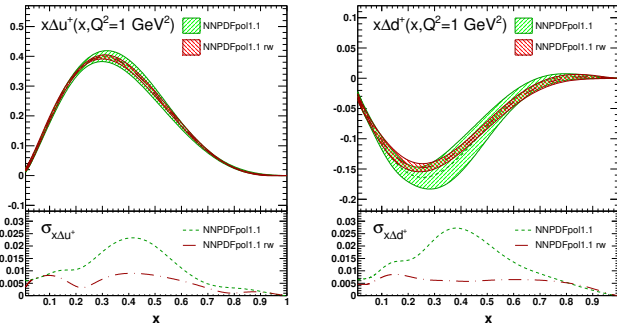
POLARIZED TO UNPOLARIZED PDF RATIOS



Model	$\Delta u^+ / u^+$	$\Delta d^+ / d^+$	Model	$\Delta u^+ / u^+$	$\Delta d^+ / d^+$
SU(6)	2/3	-1/3	NJL	0.80	-0.25
RCQM	1	-1/3	DSE (<i>realistic</i>)	0.65	-0.26
QHD ($\sigma_{1/2}$)	1	1	DSE (<i>contact</i>)	0.88	-0.33
QHD (ψ_ρ)	1	-1/3	pQCD	1	1
NNPDF ($x = 0.7$)	0.07 ± 0.05	-0.19 ± 0.34	NNPDF ($x = 0.9$)	0.61 ± 0.48	$+0.85 \pm 6.55$

Opportunities at JLAB (towards 12 GeV upgrade)

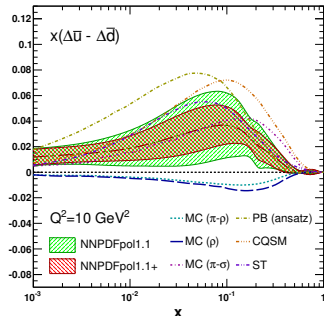
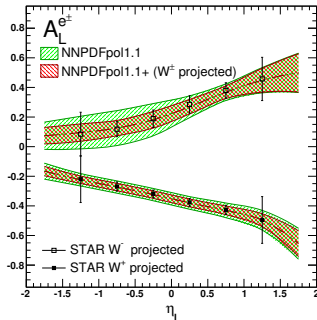
POTENTIAL IMPACT OF JLAB DATA (INCLUSIVE DIS)



Experiment	Observable	Target	N_{dat}	χ^2/N_{dat}	$\chi^2_{\text{rw}}/N_{\text{dat}}$	
JLAB E99-117	[nucl-ex/0405006]	A_1^n	He^3	3	1.22	1.02
JLAB E93-009	[nucl-ex/0605028]	A_1^p	NH^3	9	1.20	1.05
		A_1^d	ND^3	9	1.65	1.05
JLAB E06-014	[arXiv:1406.1207]	A_1^n	He^3	6	4.31	1.32
				27	1.93	1.09

Opportunities at RHIC

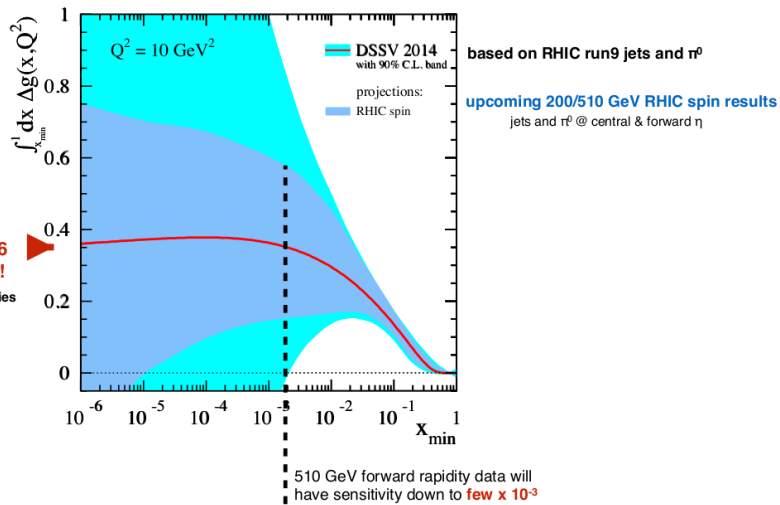
PINNING DOWN THE LIGHT POLARIZED SEA ASYMMETRY



cv	$\int_{10^{-3}}^1 dx \Delta f(x, Q^2)$		cv	$\int_{0.05}^{0.4} dx \Delta f(x, Q^2)$		
	unc (pol1.1)	unc (pol1.1+)		unc (pol1.1)	unc (pol1.1+)	
Δu^+	+0.764	± 0.035	± 0.034	+0.523	± 0.014	± 0.013
Δd^+	-0.407	± 0.037	± 0.036	-0.231	± 0.018	± 0.018
$\Delta \bar{u}$	+0.044	± 0.046	± 0.030	+0.019	± 0.023	± 0.012
$\Delta \bar{d}$	-0.088	± 0.067	± 0.032	-0.037	± 0.021	± 0.013
Δ_{sea}	+0.123	± 0.076	± 0.038	+0.056	± 0.030	± 0.016

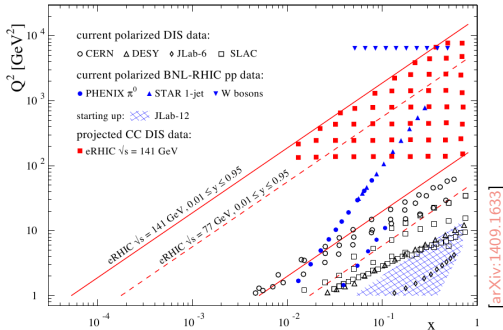
Opportunities at RHIC

PINNING DOWN THE GLUON POLARIZATION



[M. Stratmann, Talk at HiX2014]

Opportunities at a future Electron-Ion Collider



REQUIREMENTS & FEATURES

- large kinematic reach
→ high-energy collider
- precision of electromagnetic probes
→ electron beams
- spin
→ polarized hadron beams
- versatility
→ heavy ion beams

DELIVERABLES

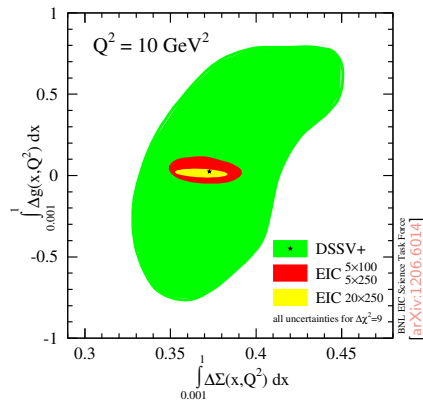
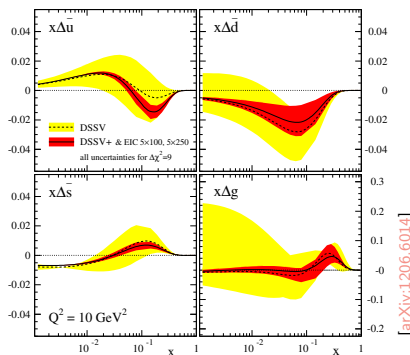
OBSERVABLES

WHAT WE LEARN

Δg	scaling violations in DIS	gluon contribution to proton spin
$\Delta q, \Delta \bar{q}$	SIDIS for pions and kaons	quark contribution to proton spin; flavor asymmetry $\Delta \bar{u} - \Delta \bar{d}$; strangeness Δs
$g_1^{W^-}, g_5^{W^-}$	inclusive CC DIS at high Q^2	flavor separation at medium x and high Q^2

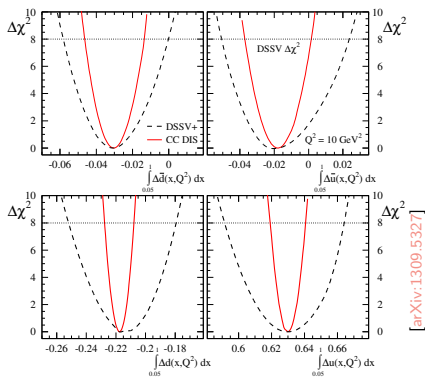
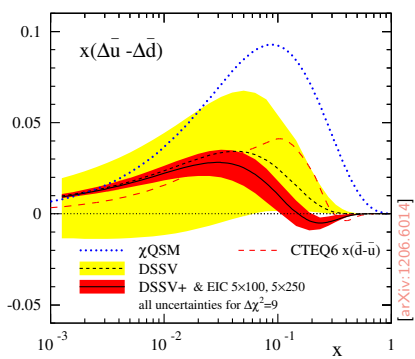
Opportunities at a future Electron-Ion Collider

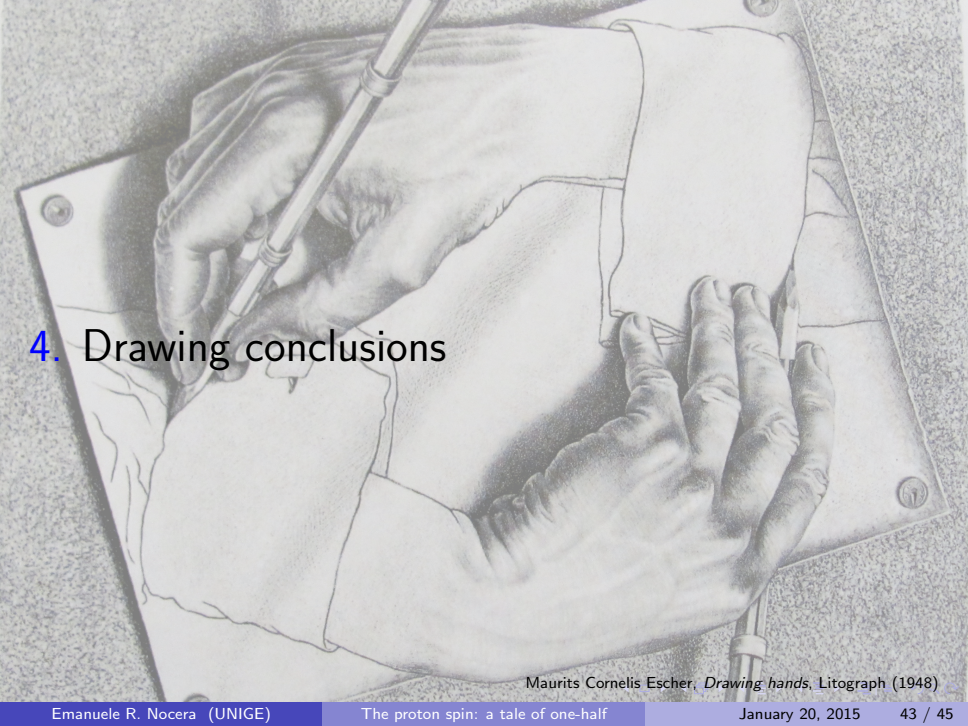
- Dramatic reduction of uncertainties of both PDFs and their moments [arXiv:1206.6014]
- Accurate determination of Δg via scaling violations in DIS [arXiv:1206.6014] [arXiv:1310.0461]
- Accurate determination of $\Delta \bar{u}$, $\Delta \bar{d}$ via SIDIS and CC DIS [arXiv:1309.5327]
- Access to unknown electroweak structure functions [arXiv:1309.5327]



Opportunities at a future Electron-Ion Collider

- Dramatic reduction of uncertainties of both PDFs and their moments [arXiv:1206.6014]
- Accurate determination of Δg via scaling violations in DIS [arXiv:1206.6014] [arXiv:1310.0461]
- Accurate determination of $\Delta \bar{u}$, $\Delta \bar{d}$ via SIDIS and CC DIS [arXiv:1309.5327]
- Access to unknown electroweak structure functions [arXiv:1309.5327]

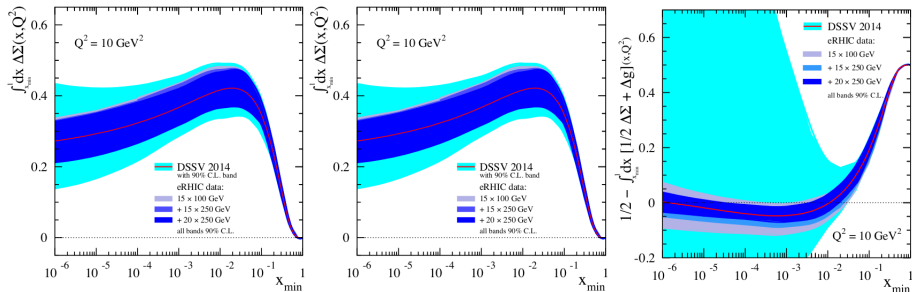




4. Drawing conclusions

Maurits Cornelis Escher, *Drawing hands*, Litograph (1948)

The ultimate spin content of the proton [arXiv:1409.1633]



After three decades of experimental and theoretical activity,
we cannot really say we know $\Delta\Sigma$ and Δg
Main culprit: small- x behavior of polarized PDFs

Spin experiments continue to produce high impact results (RHIC, JLAB, . . .)
first evidence of gluon polarization in the proton
Theory efforts and global QCD analyses try to keep up

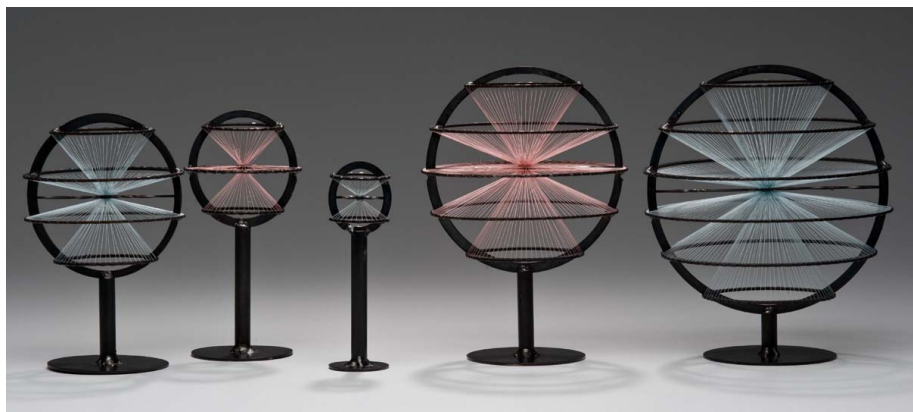
Only an EIC would be able to push forward our knowledge of nucleon spin content
Best fit results allow for zero OAM at 10 GeV²
(presumably the most precise indirect handle on OAM)

Thank you for your attention

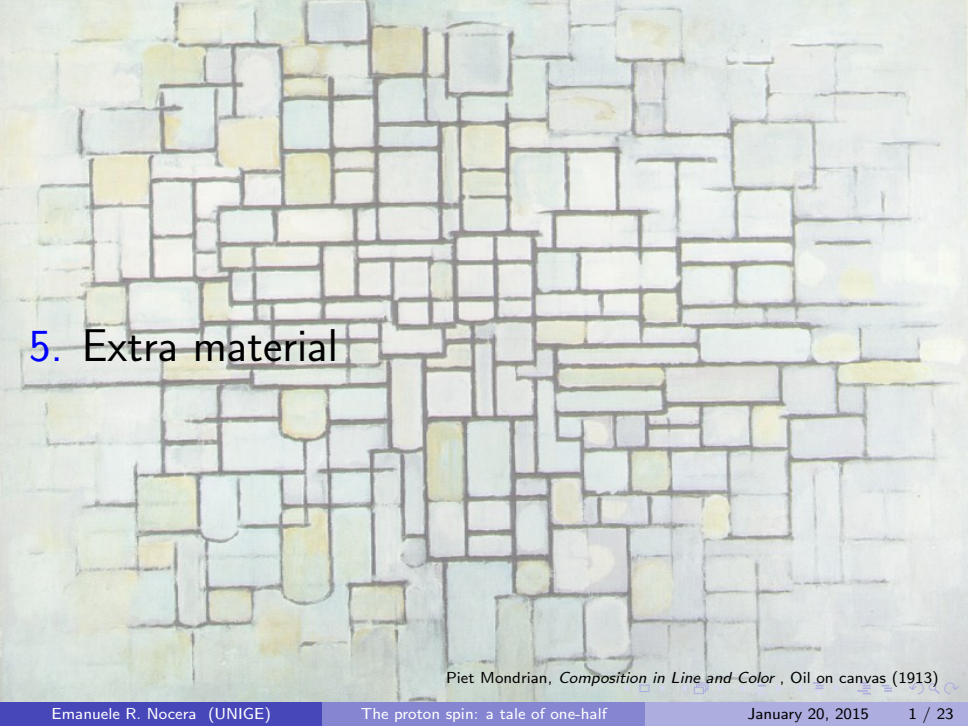
Sin-Itiro Tomonaga, Nobel Prize for Physics, 1965

[Spin] is a mysterious beast, and yet its practical effect prevails the whole of science. The existence of spin, and statistics associated with it, is the most subtle and ingenious design of Nature - without it the whole Universe would collapse.

S-I. Tomonaga, *The story of spin* 2nd ed., University of Chicago Press (1998) [from the preface]



Julian Voss-Andreae, *Spin Family (Bosons and Fermions)*, Steel and silk (2009)



5. Extra material

Piet Mondrian, *Composition in Line and Color*, Oil on canvas (1913)

The NNPDF methodology: Monte Carlo sampling

MONTE CARLO SAMPLING

- Sample the probability density $\mathcal{P}[\Delta q]$ in the space of functions assuming multi-Gaussian data probability distribution

$$g_{1,p}^{(\text{art}), (k)}(x, Q^2) = \left[1 + \sum_c r_{c,p}^{(k)} \sigma_{c,p} + r_{s,p}^{(k)} \sigma_{s,p} \right] g_{1,p}^{(\text{exp})}(x, Q^2)$$

$\sigma_{c,p}$: correlated systematics $\sigma_{s,p}$: statistical errors (also uncorrelated systematics)
 $r_{c,p}^{(k)}, r_{s,p}^{(k)}$: Gaussian random numbers

- Generate MC ensemble of N_{rep} replicas with the data probability distribution

MAIN FEATURES

- Expectation values for observables are Monte Carlo integrals

$$\langle \mathcal{O}[\Delta q] \rangle = \frac{1}{N_{\text{rep}}} \sum_{k=1}^{N_{\text{rep}}} \mathcal{O}[\Delta q_k]$$

... and the same is true for errors, correlations etc.

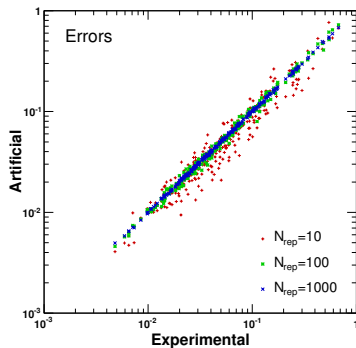
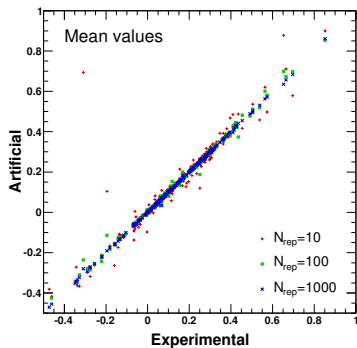
- No need to rely on linear propagation of errors
- Possibility to test for non-Gaussian behaviour in fitted PDFs

The NNPDF methodology: Monte Carlo sampling

DETERMINING THE SAMPLE SIZE

- Require the average over the replicas reproduces central values and errors of the original experimental data to desired accuracy

Qualitative approach: look at the scatter plots



Accuracy of few % requires ~ 100 replicas

The NNPDF methodology: Monte Carlo sampling

DETERMINING THE SAMPLE SIZE

- Require the average over the replicas reproduces central values and errors of the original experimental data to desired accuracy

Quantitative approach: devise proper statistical estimators

	$\left\langle \text{PE} \left[\langle g_1^{(\text{art})} \rangle \right] \right\rangle [\%]$			$r \left[g_1^{(\text{art})} \right]$		
N_{rep}	10	100	1000	10	100	1000
EMC	23.7	3.5	2.9	.76037	.99547	.99712
SMC	19.4	5.6	1.2	.94789	.99908	.99993
...

$$\left\langle \text{PE} \left[\langle F^{(\text{art})} \rangle_{\text{rep}} \right] \right\rangle_{\text{dat}} = \frac{1}{N_{\text{dat}}} \sum_{i=1}^{N_{\text{dat}}} \left| \frac{\langle F_i^{(\text{art})} \rangle_{\text{rep}} - F_i^{(\text{exp})}}{F_i^{(\text{exp})}} \right| \quad \text{Percentage Error}$$

$$r \left[F^{(\text{art})} \right] = \frac{\langle F^{(\text{exp})} \langle F^{(\text{art})} \rangle_{\text{rep}} \rangle_{\text{dat}} - \langle F^{(\text{exp})} \rangle_{\text{dat}} \langle \langle F^{(\text{art})} \rangle_{\text{rep}} \rangle_{\text{dat}}}{\sigma_s^{(\text{exp})} \sigma_s^{(\text{art})}} \quad \text{Scatter Correlation}$$

Accuracy of few % requires ~ 100 replicas

The NNPDF methodology: Monte Carlo sampling

DETERMINING THE SAMPLE SIZE

- Require the average over the replicas reproduces central values and errors of the original experimental data to desired accuracy

Quantitative approach: devise proper statistical estimators

	$\left\langle PE \left[\langle \delta g_1^{(\text{art})} \rangle \right] \right\rangle [\%]$			$r \left[\delta g_1^{(\text{art})} \right]$		
N_{rep}	10	100	1000	10	100	1000
EMC	12.8	4.9	2.0	.97397	.99521	.99876
SMC	22.4	5.4	1.7	.96585	.99489	.99980
...

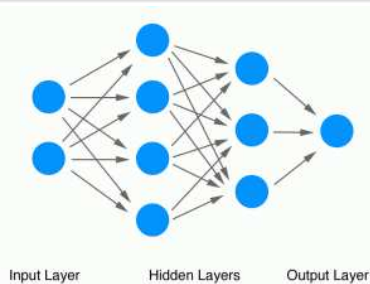
$$\left\langle PE \left[\langle F^{(\text{art})} \rangle_{\text{rep}} \right] \right\rangle_{\text{dat}} = \frac{1}{N_{\text{dat}}} \sum_{i=1}^{N_{\text{dat}}} \left| \frac{\langle F_i^{(\text{art})} \rangle_{\text{rep}} - F_i^{(\text{exp})}}{F_i^{(\text{exp})}} \right| \quad \text{Percentage Error}$$

$$r \left[F^{(\text{art})} \right] = \frac{\langle F^{(\text{exp})} \langle F^{(\text{art})} \rangle_{\text{rep}} \rangle_{\text{dat}} - \langle F^{(\text{exp})} \rangle_{\text{dat}} \langle \langle F^{(\text{art})} \rangle_{\text{rep}} \rangle_{\text{dat}}}{\sigma_s^{(\text{exp})} \sigma_s^{(\text{art})}} \quad \text{Scatter Correlation}$$

Accuracy of few % requires ~ 100 replicas

The NNPDF methodology: neural networks

A convenient **functional form**
providing **redundant** and **flexible** parametrization
used as a generator of random functions in the PDF space



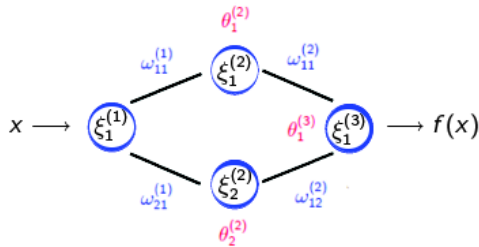
$$\xi_i^{(l)} = g \left(\sum_j^{n_l-1} \omega_{ij}^{(l-1)} \xi_j^{(l-1)} - \theta_i^{(l)} \right)$$

$$g(x) = \frac{1}{1 + e^{-x}}$$

- made of neurons grouped into layers (define the architecture)
- each neuron receives input from neurons in preceding layer (feed-forward NN)
- activation determined by parameters (**weights** and **thresholds**)
- activation determined according to a **non-linear function** (except the last layer)

The NNPDF methodology: neural networks

EXAMPLE: THE SIMPLEST 1-2-1 NN



$$f(x) \equiv \xi_1^{(3)} = \left\{ 1 + \exp \left[\theta_1^{(3)} - \frac{\omega_{11}^{(2)}}{1 + e^{\theta_1^{(2)} - x \omega_{11}^{(1)}}} - \frac{\omega_{12}^{(2)}}{1 + e^{\theta_2^{(2)} - x \omega_{21}^{(1)}}} \right] \right\}^{-1}$$

Recall:

$$\xi_i^{(l)} = g \left(\sum_j^{n_l-1} \omega_{ij}^{(l-1)} \xi_j^{(l-1)} - \theta_i^{(l)} \right) ; \quad g(x) = \frac{1}{1 + e^{-x}}$$

The NNPDF methodology: minimization and stopping

GENETIC ALGORITHM

Standard minimization unefficient owing to the large parameter space
and non-local x -dependence of the observables

Genetic algorithm provides better exploration of the whole parameter space

- Set Neural Network parameters randomly
- Make clones of the parameter vector and mutate them
- Define a **figure of merit** or error function for the k -th replica

$$E^{(k)} = \frac{1}{N_{\text{rep}}} \sum_{i,j=1}^{N_{\text{rep}}} \left(g_{1,i}^{(\text{art})(k)} - g_{1,i}^{(\text{net})(k)} \right) \left((\text{cov})^{-1} \right)_{ij} \left(g_{1,j}^{(\text{art})(k)} - g_{1,j}^{(\text{net})(k)} \right)$$

$g_{1,i}^{(\text{art})(k)}$: generated from Monte Carlo sampling

$g_{1,i}^{(\text{net})(k)}$: computed from Neural Network PDFs

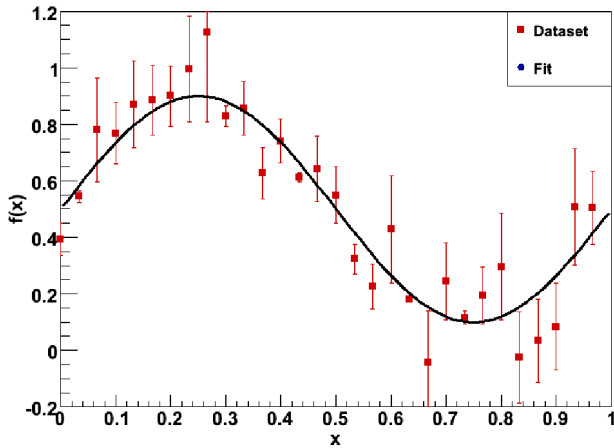
- Select the best set of parameters and perform other manipulations (crossing, mutating, ...) until stability is reached.

The NNPDF methodology: minimization and stopping

DRAWBACK

- NN can learn fluctuations owing to their flexibility

UNDERLYING PHYSICAL LAW

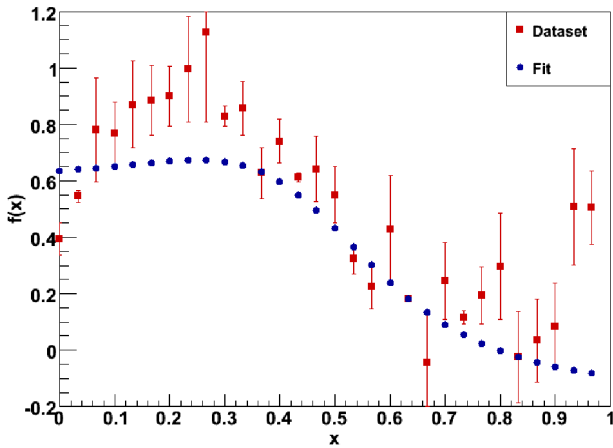


The NNPDF methodology: minimization and stopping

DRAWBACK

- NN can learn fluctuations owing to their flexibility

UNDERLEARNING

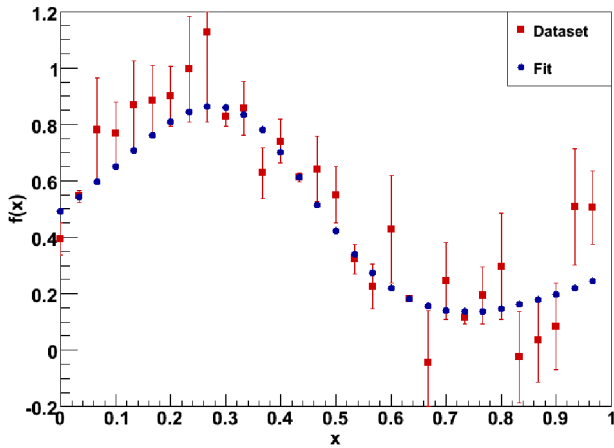


The NNPDF methodology: minimization and stopping

DRAWBACK

- NN can learn fluctuations owing to their flexibility

PROPER LEARNING

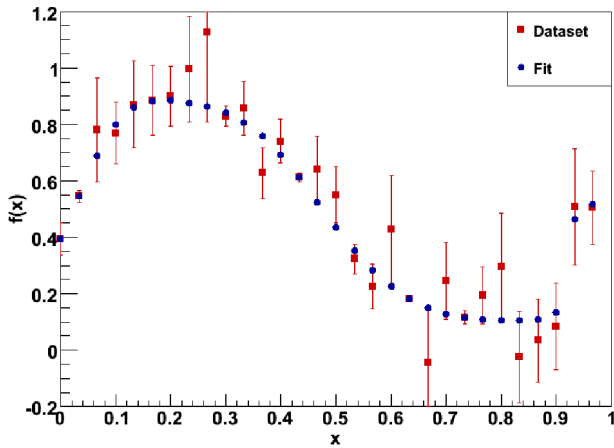


The NNPDF methodology: minimization and stopping

DRAWBACK

- NN can learn fluctuations owing to their flexibility

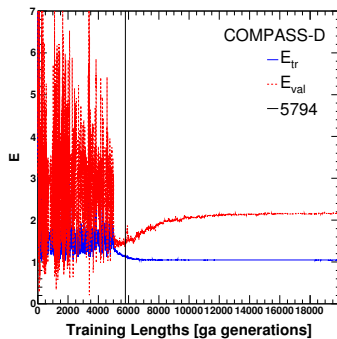
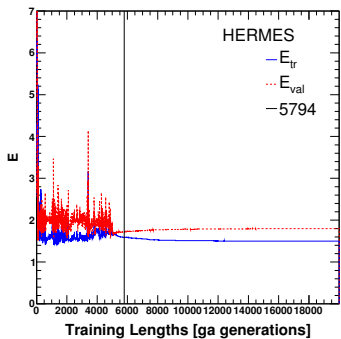
OVERLEARNING



The NNPDF methodology: minimization and stopping

CROSS-VALIDATION METHOD

- divide data into two subsets (**training & validation**)
- train the NN on training subset and compute χ^2 for each subset
- stop when χ^2 of validation subset no longer decreases (NN are learning noise!)



The best fit does not coincide with the χ^2 absolute minimum

The NNPDF methodology: reweighting

[arXiv:1012.0836] [arXiv:1108.1758]

- ① We would like to assess the impact of including a **new data set** $\{y\} = \{y_1, \dots, y_n\}$ (delivered with σ_{ij}) in a **prior ensemble** of PDF replicas $\{f_k\}$, $k = 1, \dots, N_{\text{rep}}$
- ② We can apply **Bayes theorem** to determine the conditional probability of PDF upon inclusion of the new data and update the probability density in the space of PDFs

$$\mathcal{P}_{\text{new}} = \mathcal{N}_x \mathcal{P}(\chi_k^2 | \{f_k\}) \mathcal{P}_{\text{old}}(\{f_k\}) \quad \mathcal{P}(\chi_k^2 | \{f_k\}) = [\chi_k^2(\{y\}, \{f_k\})]^{\frac{1}{2}(n-1)} e^{-\frac{1}{2}\chi_k^2(\{y\}, \{f_k\})}$$

$$\chi_k^2(\{y\}, \{f_k\}) = \sum_{i,j}^n \{y_i - y_i[f_k]\} \sigma_{ij} \{y_j - y_j[f_k]\}$$

- ③ Replicas are **no longer equally probable**. Expectation values are given by

$$\langle \mathcal{O}[f_i(x, Q^2)] \rangle_{\text{new}} = \sum_{k=1}^{N_{\text{rep}}} w_k \mathcal{O}[f_i^{(k)}(x, Q^2)]$$

$$w_k \propto [\chi_k^2(\{y\}, \{f_k\})]^{\frac{1}{2}(n-1)} e^{-\frac{1}{2}\chi_k^2(\{y\}, \{f_k\})} \quad \text{with} \quad N_{\text{rep}} = \sum_{k=1}^{N_{\text{rep}}} w_k$$

Reweighting allows to incorporate new datasets **without** need of **refitting**

The NNPDF methodology: unweighting [arXiv:11081758]

Unweighting allows for constructing an ensemble of equally probable PDFs statistically equivalent to a given reweighted set
Hence, the new set can be given without weights

IDEA

Given a weighted set of N_{rep} replicas, select (possibly more than once) replicas carrying relatively high weight and discard replicas carrying relatively small weight

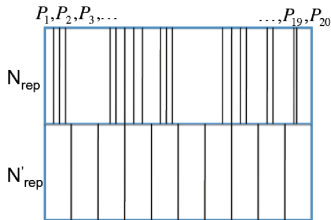
CONSTRUCTION OF THE UNWEIGHTED SET

- ① Set the number of replicas N'_{rep} in the unweighted set
(pointless to choose $N'_{\text{rep}} > N_{\text{rep}}$: no gain of information)
- ② Compute, for the k -th replica of the reweighted set, the integer number

$$w'_k = \sum_{j=1}^{N'_{\text{rep}}} \theta\left(\frac{j}{N'_{\text{rep}}} - P_{k-1}\right) \theta\left(P_k - \frac{j}{N'_{\text{rep}}}\right), \quad P_k = \sum_{j=0}^k \frac{w_j}{N_{\text{rep}}}, \quad \sum_{k=1}^{N_{\text{rep}}} w'_k = N'_{\text{rep}}$$

- ③ Construct the unweighted set taking w'_k copies of the k -th replica, $k = 1, \dots, N_{\text{rep}}$

The NNPDF methodology: unweighting [arXiv:11081758]



CONSTRUCTION OF THE UNWEIGHTED SET

- ① Set the number of replicas N'_{rep} in the unweighted set
(pointless to choose $N'_{\text{rep}} > N_{\text{rep}}$: no gain of information)
- ② Compute, for the k -th replica of the reweighted set, the integer number

$$w'_k = \sum_{j=1}^{N'_{\text{rep}}} \theta\left(\frac{j}{N'_{\text{rep}}} - P_{k-1}\right) \theta\left(P_k - \frac{j}{N'_{\text{rep}}}\right), \quad P_k = \sum_{j=0}^k \frac{w_j}{N_{\text{rep}}}, \quad \sum_{k=1}^{N_{\text{rep}}} w'_k = N'_{\text{rep}}$$

- ③ Construct the unweighted set taking w'_k copies of the k -th replica, $k = 1, \dots, N_{\text{rep}}$

The NNPDF methodology: closure test [arXiv:1410.8849]

Validation and optimization of fitting strategy
performed on closure test with known underlying physical law

- ① Set the theory (e.g. NLO pQCD)
- ② Set the fitting methodology (e.g. genetic algorithm, cross-validation)
- ③ Set the underlying *true* physical law (e.g. input PDFs from MSTW08)
- ④ Generate pseudodata and perform the fit with given theory and methodology
- ⑤ Validate the resulting PDF set
 - reproduce the underlying law (both central value and uncertainties)
 - check the consistency of expected values of χ^2
 - check that PDF reweighting is equal to PDF refitting (Bayesian inference)
 - level 0: fluctuations on pseudodata ; Monte Carlo replica generation
 - level 1: fluctuations on pseudodata ; Monte Carlo replica generation
 - level 2: fluctuations on pseudodata ; Monte Carlo replica generation

Full control of procedural uncertainties

NNPDFpol1.1: fit quality

Experiment	N_{dat}	χ^2/N_{dat}	NNPDFpol1.0	χ^2/N_{dat}	NNPDFpol1.1
EMC	10	0.44		0.43	
SMC	24	0.93		0.90	
SMClowx	16	0.97		0.97	
E143	50	0.64		0.67	
E154	11	0.40		0.45	
E155	40	0.89		0.85	
COMPASS-D	15	0.65		0.70	
COMPASS-P	15	1.31		1.38	
HERMES97	8	0.34		0.34	
HERMES	56	0.79		0.82	
	245	0.77		0.78	
COMPASS (OC)	45	—		1.22	
STAR (jets)	41	—		1.05	
PHENIX (jets)	6	—		0.24	
STAR- A_L	24	—		0.72	
STAR- A_{LL}	12	—		0.75	
	373	—		1.05	

NNPDFpol1.1: open-charm production at COMPASS

$$A^{\gamma N \rightarrow D^0 X} = \frac{\Delta g \otimes \Delta \hat{\sigma}_{\gamma g} \otimes D_c^H}{g \otimes \hat{\sigma}_{\gamma g} \otimes D_c^H}$$

Virtual photon-nucleon asymmetry for open-charm production

[arXiv:1212.1319]

FEATURES

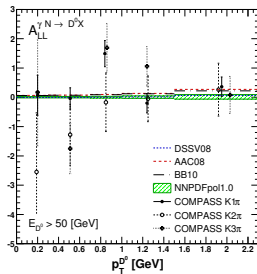
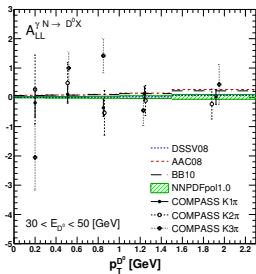
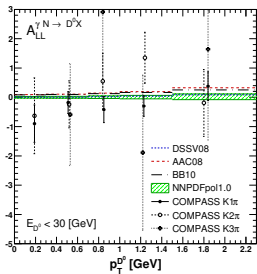
- Δg is probed *directly* through the photon-gluon fusion process
(in DIS Δg is mostly probed through scaling violations instead)
- the fragmentation functions for heavy quarks are computable in perturbation theory
(and only introduce a very moderate uncertainty in the fit)

EXPERIMENTAL MEASUREMENT

- COMPASS (2002-2007) [arXiv:1211.6849]

Experiment	Set	N_{dat}	NNPDFpol1.0	χ^2/N_{dat} DSSV08	AAC08	BB10
COMPASS		45	1.23	1.23	1.27	1.25
	COMPASS $K1\pi$	15	1.27	1.27	1.43	1.38
	COMPASS $K2\pi$	15	0.51	0.51	0.56	0.55
	COMPASS $K3\pi$	15	1.90	1.90	1.81	1.82

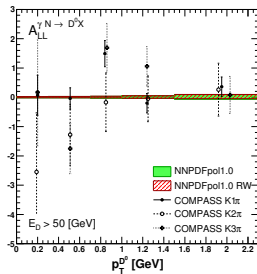
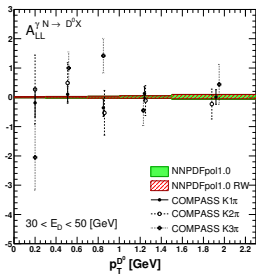
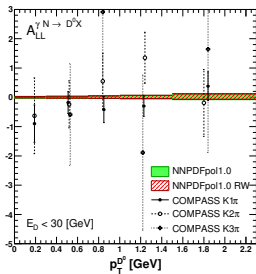
NNPDFpol1.1: open-charm production at COMPASS



Data are affected by large uncertainties w.r.t. the uncertainty due to PDFs
 They do not show a clear trend

Experiment	Set	N_{dat}	NNPDFpol1.0	χ^2/N_{dat}	DSSV08	AAC08	BB10
COMPASS		45	1.23	1.23	1.27	1.25	
	COMPASS $K1\pi$	15	1.27	1.27	1.43	1.38	
	COMPASS $K2\pi$	15	0.51	0.51	0.56	0.55	
	COMPASS $K3\pi$	15	1.90	1.90	1.81	1.82	

NNPDFpol1.1: open-charm production at COMPASS



The impact of open-charm data from COMPASS is mostly negligible, as we notice from the value of the χ^2/N_{ndat} and the reweighted observable

Experiment	Set	N_{dat}	χ^2/N_{dat}	$\chi^2_{\text{rw}}/N_{\text{dat}}$
COMPASS		45	1.23	1.23
	COMPASS $K1\pi$	15	1.27	1.27
	COMPASS $K2\pi$	15	0.51	0.51
	COMPASS $K3\pi$	15	1.90	1.89

NNPDFpol1.1: inclusive jet production at RHIC

$$A_{LL}^{1jet} = \frac{\sigma^{++} - \sigma^{+-}}{\sigma^{++} + \sigma^{+-}}$$

Longitudinal double-spin asymmetry for single-inclusive jet production

[arXiv:hep-ph/9808262] [arXiv:hep-ph/0404057] [arXiv:1209.1785]

FEATURES

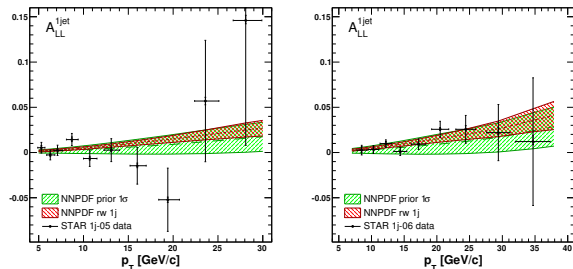
- sensitive to the polarized gluon Δg
(receives leading contribution from $gq \rightarrow qg$ and $qg \rightarrow qg$ partonic subprocesses)

EXPERIMENTAL MEASUREMENT

- STAR 2005, 2006 [arXiv:1205.2735], 2009 [arXiv:1405.5134]
- PHENIX [arXiv:1009.4921] at RHIC

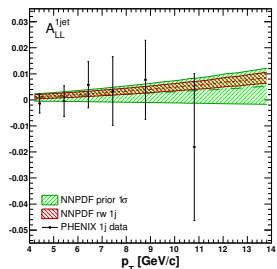
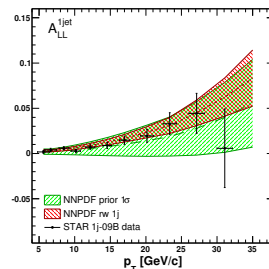
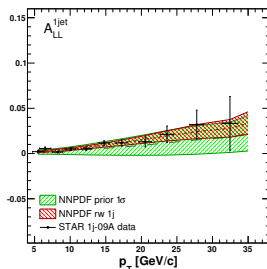
Data set	N_{dat}	jet-algorithm	R	$[\eta_{\min}, \eta_{\max}]$	\sqrt{s} [GeV]	\mathcal{L} [pb^{-1}]
STAR 1j-05	10	midpoint-cone	0.4	[+0.20, +0.80]	200	2.1
STAR 1j-06	9	midpoint-cone	0.7	[-0.70, +0.90]	200	5.5
STAR 1j-09A	11	anti- k_t	0.6	[-0.50, +0.50]	200	25
STAR 1j-09B	11	anti- k_t	0.6	[-1.00, -0.50] [+0.50, +1.00]	200	25
PHENIX 1j	6	seeded-cone	0.3	[-0.35, +0.35]	200	2.1

NNPDFpol1.1: inclusive jet production at RHIC



Experiment	Set	N_{dat}	χ^2 / N_{dat}				$\chi^2_{\text{rw}} / N_{\text{dat}}$			
			1σ	2σ	3σ	4σ	1σ	2σ	3σ	4σ
STAR		41	1.50	1.49	1.50	1.50	1.05	1.04	1.04	1.04
	STAR 1j-05	10	1.04	1.05	1.04	1.04	1.01	1.02	1.02	1.02
	STAR 1j-06	9	0.75	0.76	0.76	0.76	0.59	0.58	0.59	0.59
	STAR 1j-09A	11	1.40	1.39	1.39	1.40	0.98	0.99	0.98	0.98
	STAR 1j-09B	11	3.04	3.05	3.03	3.05	1.18	1.17	1.17	1.18
PHENIX	PHENIX 1j	6	0.24	0.24	0.24	0.24	0.24	0.24	0.24	0.24
		47	1.35	1.35	1.35	1.36	1.00	1.01	1.01	1.00

NNPDFpol1.1: inclusive jet production at RHIC



Experiment	Set	N_{dat}	χ^2 / N_{dat}				$\chi^2_{\text{rw}} / N_{\text{dat}}$			
			1σ	2σ	3σ	4σ	1σ	2σ	3σ	4σ
STAR		41	1.50	1.49	1.50	1.50	1.05	1.04	1.04	1.04
	STAR 1j-05	10	1.04	1.05	1.04	1.04	1.01	1.02	1.02	1.02
	STAR 1j-06	9	0.75	0.76	0.76	0.76	0.59	0.58	0.59	0.59
	STAR 1j-09A	11	1.40	1.39	1.39	1.40	0.98	0.99	0.98	0.98
	STAR 1j-09B	11	3.04	3.05	3.03	3.05	1.18	1.17	1.17	1.18
PHENIX	PHENIX 1j	6	0.24	0.24	0.24	0.24	0.24	0.24	0.24	0.24
		47	1.35	1.35	1.35	1.36	1.00	1.01	1.01	1.00

NNPDFpol1.1: W^\pm production at RHIC

$$A_L^{W^\pm} = \frac{\sigma^+ - \sigma^-}{\sigma^+ + \sigma^-}$$

$$A_{LL}^{W^\pm} = \frac{\sigma^{++} - \sigma^{+-}}{\sigma^{++} + \sigma^{+-}}$$

$$A_L^{W^+} \sim \frac{\Delta u(x_1)\bar{d}(x_2) - \Delta \bar{d}(x_1)u(x_2)}{u(x_1)\bar{d}(x_2) + \bar{d}(x_1)u(x_2)}$$

$$A_L^{W^-} \sim \frac{\Delta d(x_1)\bar{u}(x_2) - \Delta \bar{u}(x_1)d(x_2)}{d(x_1)\bar{u}(x_2) + \bar{u}(x_1)d(x_2)}$$

Longitudinal single-spin asymmetry for W^\pm boson production

[arXiv:1003.4533]

FEATURES

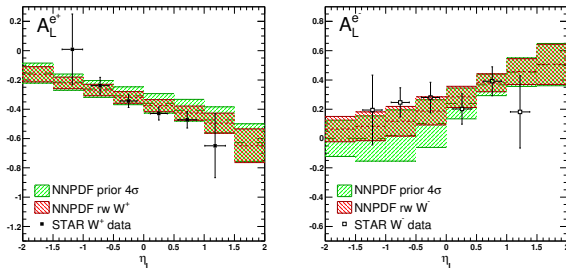
- sensitive to individual quark and antiquark flavours ($\Delta u, \Delta \bar{u}, \Delta d, \Delta \bar{d}$)
(purely weak process coupling q_L with \bar{q}_R at partonic level, $u_L\bar{d}_R \rightarrow W^+$ or $d_L\bar{u}_R \rightarrow W^-$)
- no need for fragmentation functions (instead of SIDIS)

EXPERIMENTAL MEASUREMENT

- STAR and PHENIX at RHIC [arXiv:1009.0326] [arXiv:1009.0505] [arXiv:1404.6880]

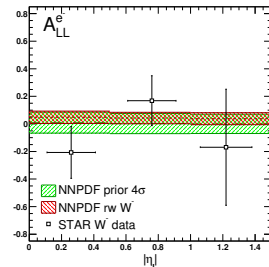
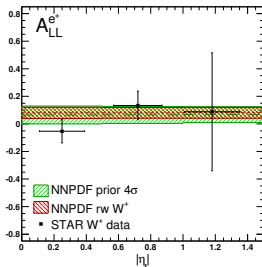
Data set	N_{dat}	$[\rho_T, \min, \rho_T, \max]$ [GeV]	\sqrt{s} [GeV]	\mathcal{L} [pb^{-1}]
STAR- W^+ (prel.)	6	[25, 50]	510	72
STAR- W^- (prel.)	6	[25, 50]	510	72

NNPDFpol1.1: W^\pm production at RHIC



Experiment	Set	N_{dat}	χ^2/N_{dat}				$\chi^2_{\text{rw}}/N_{\text{dat}}$			
			1σ	2σ	3σ	4σ	1σ	2σ	3σ	4σ
STAR- A_L		12	1.38	1.44	1.39	1.33	1.08	0.88	0.74	0.74
	STAR- $A_L^{W^+}$	6	0.75	0.75	0.86	0.90	0.75	0.75	0.68	0.70
	STAR- $A_L^{W^-}$	6	1.92	2.03	1.82	1.67	1.32	1.08	0.83	0.82
STAR-ALL		6	0.82	0.81	0.78	0.78	0.82	0.80	0.76	0.76
	STAR- $A_{LL}^{W^+}$	3	0.92	0.88	0.81	0.80	0.90	0.85	0.77	0.76
	STAR- $A_{LL}^{W^-}$	3	0.73	0.74	0.75	0.76	0.73	0.74	0.75	0.76
		18	1.19	1.20	1.15	1.15	1.00	0.87	0.78	0.77

NNPDFpol1.1: W^\pm production at RHIC

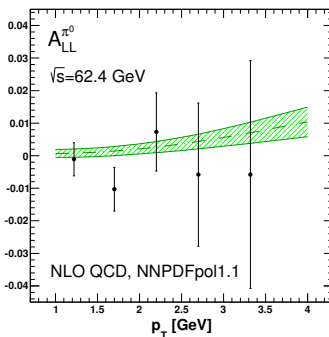
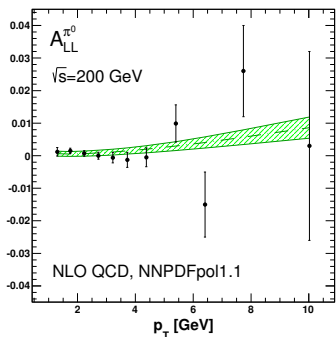


Experiment	Set	N_{dat}	χ^2/N_{dat}				$\chi^2_{\text{rw}}/N_{\text{dat}}$			
			1σ	2σ	3σ	4σ	1σ	2σ	3σ	4σ
STAR- A_L		12	1.38	1.44	1.39	1.33	1.08	0.88	0.74	0.74
	STAR- $A_L^{W^+}$	6	0.75	0.75	0.86	0.90	0.75	0.75	0.68	0.70
	STAR- $A_L^{W^-}$	6	1.92	2.03	1.82	1.67	1.32	1.08	0.83	0.82
STAR-ALL		6	0.82	0.81	0.78	0.78	0.82	0.80	0.76	0.76
	STAR- $A_{LL}^{W^+}$	3	0.92	0.88	0.81	0.80	0.90	0.85	0.77	0.76
	STAR- $A_{LL}^{W^-}$	3	0.73	0.74	0.75	0.76	0.73	0.74	0.75	0.76
		18	1.19	1.20	1.15	1.15	1.00	0.87	0.78	0.77

NNPDFpol1.1: single-hadron production at RHIC

$$A_{LL}^H = \frac{\sigma^{++} - \sigma^{+-}}{\sigma^{++} + \sigma^{+-}} = \frac{\sum_{a,b,c=q,\bar{q},g} f_a \otimes f_b \otimes D_c^H \otimes \Delta\hat{\sigma}_{ab}^c}{\sum_{a,b,c=q,\bar{q},g} f_a \otimes f_b \otimes D_c^H \otimes \hat{\sigma}_{ab}^c}$$

PHENIX [arXiv:0810.0701] [arXiv:0810.0694] [arXiv:1402.6296] STAR [arXiv:1309.1800]

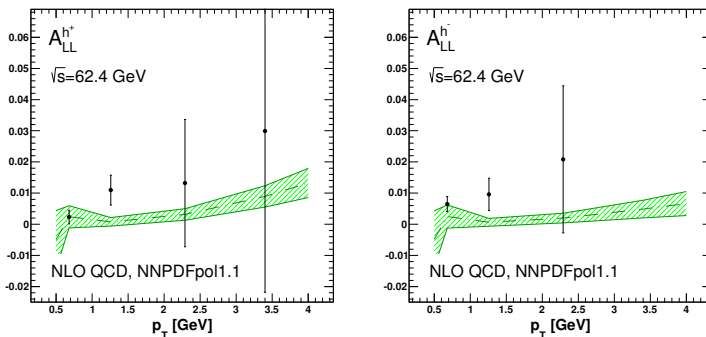


- Good agreement between experimental data and theoretical predictions
- Experimental uncertainties are larger than those of the corresponding predictions
- We expect a slight impact on the gluon PDF from these data

NNPDFpol1.1: single-hadron production at RHIC

$$A_{LL}^H = \frac{\sigma^{++} - \sigma^{+-}}{\sigma^{++} + \sigma^{+-}} = \frac{\sum_{a,b,c=q,\bar{q},g} f_a \otimes f_b \otimes D_c^H \otimes \Delta\hat{\sigma}_{ab}^c}{\sum_{a,b,c=q,\bar{q},g} f_a \otimes f_b \otimes D_c^H \otimes \hat{\sigma}_{ab}^c}$$

PHENIX [arXiv:0810.0701] [arXiv:0810.0694] [arXiv:1402.6296] STAR [arXiv:1309.1800]

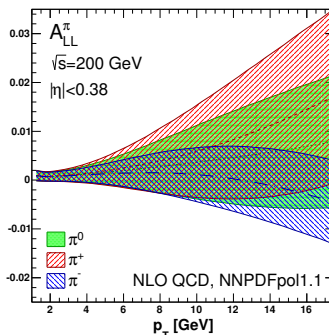
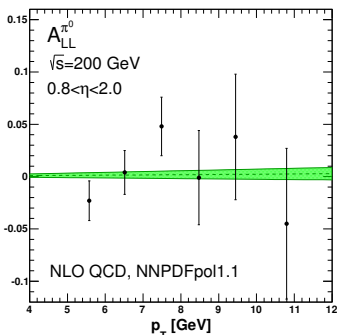


- Good agreement between experimental data and theoretical predictions
- Experimental uncertainties are larger than those of the corresponding predictions
- We expect a slight impact on the gluon PDF from these data

NNPDFpol1.1: single-hadron production at RHIC

$$A_{LL}^H = \frac{\sigma^{++} - \sigma^{+-}}{\sigma^{++} + \sigma^{+-}} = \frac{\sum_{a,b,c=q,\bar{q},g} f_a \otimes f_b \otimes D_c^H \otimes \Delta\hat{\sigma}_{ab}^c}{\sum_{a,b,c=q,\bar{q},g} f_a \otimes f_b \otimes D_c^H \otimes \hat{\sigma}_{ab}^c}$$

PHENIX [arXiv:0810.0701] [arXiv:0810.0694] [arXiv:1402.6296] STAR [arXiv:1309.1800]

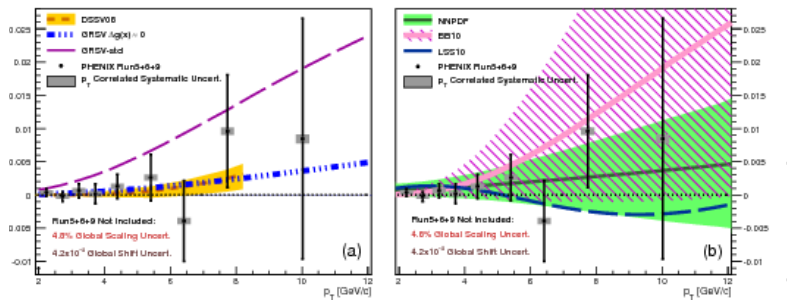


- Good agreement between experimental data and theoretical predictions
- Experimental uncertainties are larger than those of the corresponding predictions
- We expect a slight impact on the gluon PDF from these data

NNPDFpol1.1: single-hadron production at RHIC

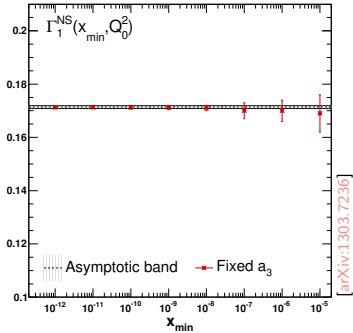
$$A_{LL}^H = \frac{\sigma^{++} - \sigma^{+-}}{\sigma^{++} + \sigma^{+-}} = \frac{\sum_{a,b,c=q,\bar{q},g} f_a \otimes f_b \otimes D_c^H \otimes \Delta\hat{\sigma}_{ab}^c}{\sum_{a,b,c=q,\bar{q},g} f_a \otimes f_b \otimes D_c^H \otimes \hat{\sigma}_{ab}^c}$$

PHENIX [arXiv:0810.0701] [arXiv:0810.0694] [arXiv:1402.6296] STAR [arXiv:1309.1800]

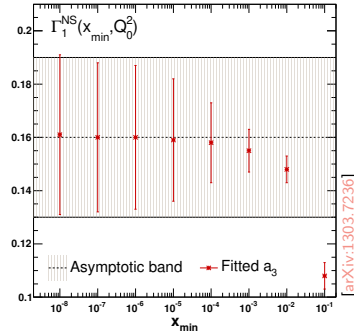


- Good agreement between experimental data and theoretical predictions
- Experimental uncertainties are larger than those of the corresponding predictions
- We expect a slight impact on the gluon PDF from these data

Open issues: the Bjorken sum rule



$$\text{fixed } a_3 = 1.2701 \pm 0.0025$$

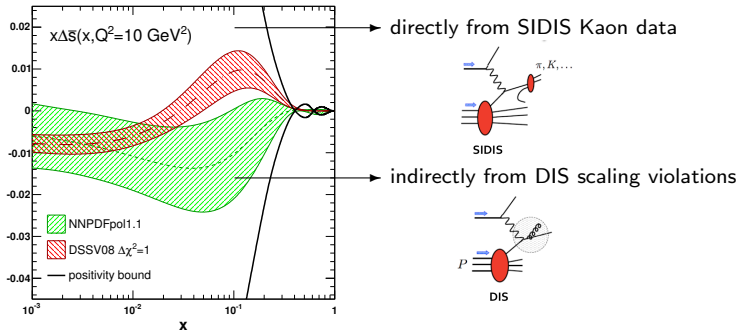


$$\text{fitted } a_3 = 1.19 \pm 0.22$$

$$\begin{aligned} \Gamma_1^{\text{NS}}(x_{\min}, Q^2) &\equiv \int_{x_{\min}}^1 dx [g_1^p(x, Q^2) - g_1^n(x, Q^2)] \xrightarrow{x_{\min}=0} \frac{1}{6} a_3(Q^2) \Delta C_{\text{NS}}[\alpha_s(Q^2)] \\ a_3(Q^2) &= \int_0^1 dx [\Delta u(x, Q^2) + \Delta \bar{u}(x, Q^2) - \Delta d(x, Q^2) - \Delta \bar{d}(x, Q^2)] \end{aligned}$$

Open issues: the strange content of the proton

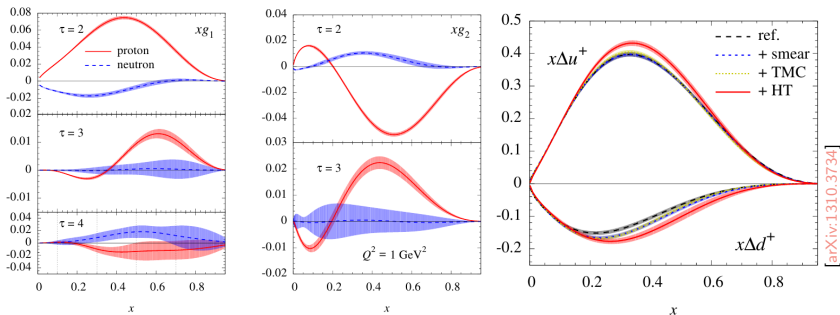
$\Delta\bar{s}$ (assuming $\Delta s = \Delta\bar{s}$, which may not be true [[hep-ph/0505153](#)])



NNPDFpol1.1: DIS , SIDIS (K^\pm) ;
DSSV08: DIS , SIDIS (K^\pm) ;

- DIS data \Rightarrow negative $x\Delta\bar{s}$; SIDIS data \Rightarrow changing-sign $x\Delta\bar{s}$
- New, very precise, JLAB data (DIS) point to negative $x\Delta s$ [[arXiv:1410.1657](#)]
- Is there mounting tension between DIS and SIDIS data?
- How well do we know K fragmentation functions? [[arXiv:1103.5979](#)]

Progress on inclusion of higher-twist corrections: JAM13



[arXiv:1310.3734]

- leading-twist factorization of g_1 and g_2 receives contributions from higher-twist terms

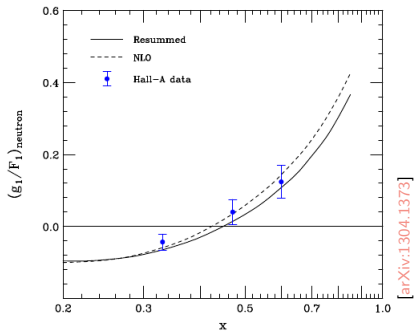
$$g_1 = g_1^{\tau=2} + g_1^{\tau=3} + g_1^{\tau=4} \quad g_2 = g_2^{\tau=2} + g_2^{\tau=3}$$

- $g_2^{\tau=2}$ can be related to $g_1^{\tau=2}$ via Wandzura-Wilczek relation [PLB,72,195]
- $g_2^{\tau=3}$ can be related to $g_1^{\tau=3}$ via Blümlein-Tkablage identity [arXiv:hep-ph/9812478]
- $g_2^{\tau=3}$ can be parametrized (using e.g. the form by Braun et al.) [arXiv:1103.1269]
- $g_1^{\tau=4}$ can be parametrized as $g_1^{\tau=4}(x, Q^2) = h(x)/Q^2$ (D. Hui)

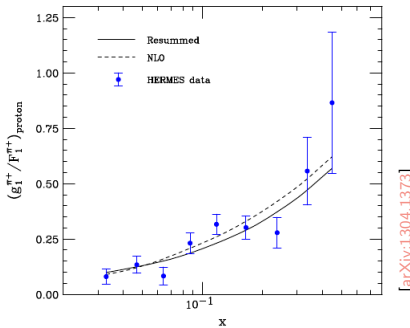
- higher twists to both g_1 and g_2 are included in JAM13
- higher twist contributions are sizable and are needed for describing JLAB data properly

Progress on all-order resummation

DIS: Hall A data [arXiv:nucl-ex/0405006]



SIDIS: G. Karayan data [arXiv:hep-ex/0407032]

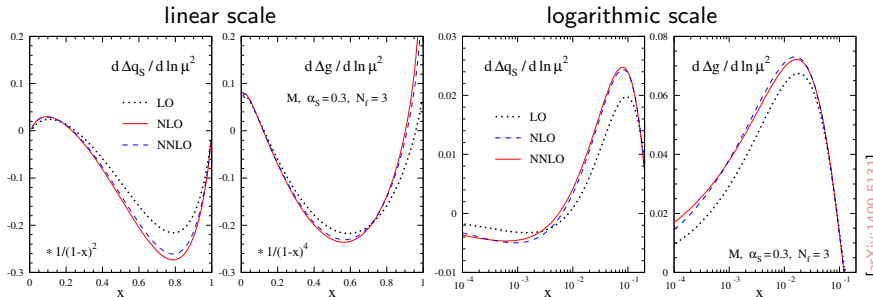


[arXiv:1304.1373]

[arXiv:1304.1373]

- resummation of large logarithm corrections to spin asymmetries in DIS and SIDIS
- asymmetries are rather insensitive to the inclusion of resummed higher-order terms
- modest decrease of spin asymmetries at fairly high x values, more pronounced for SIDIS
- most relevant for JLAB kinematics, important for future high statistic JLAB12

Progress on higher-order computations ($\overline{\text{MS}}$ scheme)



- NNLO (three-loop) corrections to spin-dependent splitting functions have been computed
- NNLO corrections to the splitting functions are small outside the region of small x
- corrections to the evolution of the PDFs can be unproblematic down to $x \approx 10^{-4}$
- QCD analyses of polarized PDFs are now feasible up to NNLO accuracy
 - only in a FFN scheme (VFN would require non-trivial unknown matching conditions)
 - only including DIS data (coefficient functions are known at NNLO only for DIS)

[arXiv:1409.5131]